EMBRY-RIDDLE
Aeronautical University™

SCHOLARLY COMMONS

Dissertations and Theses

12-2016

Configuration Validation of a Novel In-Space Propellant Storage and Transfer System

Priyadarshan Sundararaju

CONFIGURATION VALIDATION OF A NOVEL IN-SPACE PROPELLANT

STORAGE AND TRANSFER SYSTEM

A Thesis

Submitted to the Faculty

of

Embry-Riddle Aeronautical University

by

Priyadarshan Sundararaju

In Partial Fulfillment of the

Requirements for the Degree

of

Master of Science in Aerospace Engineering

December 2016

Embry-Riddle Aeronautical University
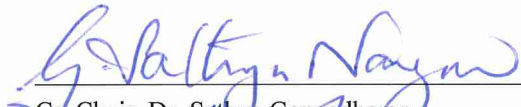
Daytona Beach, Florida

CONFIGURATION VALIDATION OF A NOVEL IN-SPACE PROPELLANT STORAGE AND TRANSFER SYSTEM

by

Priyadarshan Sundararaju

A Thesis prepared under the direction of the candidate's committee chairman, Dr. Sathya Gangadharan, Department of Mechanical Engineering, and has been approved by the members of the thesis committee. It was submitted to the School of Graduate Studies and Research and was accepted in partial fulfillment of the requirements for the degree of Master of Science in Aerospace Engineering.

THESIS COMMITTEE

Co-Chair, Dr. Sathya Gangadharan

Co-Chair, Dr. Sirish Namilae

Member, Dr. Laksh Narayanaswami

Graduate Program Coordinator, Dr. Magdy Attia

12-6-2016
Date

Dean of College of Engineering, Dr. Maj Mirmirani

12/7/2016
Date

Vice Chancellor, Academic Support, Dr. Christopher Grant

12/7/16
Date

ACKNOWLEDGMENTS

TABLE OF CONTENTS

LIST OF TABLES

LIST OF FIGURES

SYMBOLS

m	Mass
v	Velocity
F	Force
g	Gravity
x	Center of mass
h	Height
ρ	Density
r	Radius
T_r	Total kinetic Energy
H_G	Torque free rotation
M_I	Moment of inertia
H_w	Total frequency
O_w	Resonant frequency
I_w	Output frequency
?	Dynamic viscosity
?	Time
?	Amplitude
?	Frequency
?	Coefficient of stiffness
$?_?$	Permeability of vacuum
N	Number of turns in electromagnet
I	Current
A	Area

ABBREVIATIONS

LEO	Low Earth Orbit
GSO	Geo-Synchronous Orbit
CLV's	Commercial Launch Vehicles
EVA	Extravehicular-Activities
CAD	Computer aided design
FRF	Frequency Response Function
FFT	Fast Fourier Transform
CFD	Computational Fluid Dynamics
DAQ	Data Acquisition
MATLAB	Matrix Laboratory
CATIA	Computer Aided Three-Dimensional Interactive Application
3D	3-Dimensional
RANS	Reynolds-Averaged Navier-Stokes equation

ABSTRACT

The concept of developing a new technology for on-orbit storage and refueling system has been a great interest among scientists for many decades. This study is about Centaur-based on-orbit propellant storage and transfer. This system takes the advantage of rotational settling to a simple fluid management (FM) system. Specifically, enabling settled fluid transfer and settled pressure control between two tanks. This thesis work focuses on configuration and validation of static and dynamic stability, mass gauging and CFD analysis of the rotational propellant transfer method in space. The application of this technology in Low Earth Orbit (LEO) and Geo-Synchronous Orbit (GEO) would enable further extending the mission capabilities of modern day Commercial Launch Vehicles (CLV'S). Bulk Storage and handling of propellant liquids in space involves considerable technical challenge due to high vacuum and potential zero gravity environment. In order to raise the technology readiness level of this system, experimental study was conducted on (a) system dynamics, (b) mass gauging, (c) CFD analysis. The stability dynamics study showed the system to be stable about the minor axis with high rotational velocity. The mass gauging system was validated using experimental modal analysis. CFD analysis was used to analysis the fluid behavior during the transfer. These results provide a critical insight into the behavior and physical tendencies of the on-orbit refueling system.

1. Introduction

Suborbital fuel transfer is a challenging but necessary technology needed for deep space missions. Developing this type of technology has its technical difficulties. Fuel transfer in space will be primarily dependent on the space mission, and the transfer system would depend upon the mission application. The most feasible concept for transferring small amount of storable propellants might differ radically from that which is suitable for the transfer of large amount of liquid cryogens. Another important consideration is whether the transfer operation is carried out under zero-g conditions or whether an artificial gravity has to be created. Various concepts has been described below along with their compatibility with typical orbital refueling requirements.

The transfer of propellants on Earth orbit is a complex task. It includes all the operations normally involved in launching a vehicle into a given orbital attitude and inclination. Additionally, it also involves the rendezvousing and docking of the supply tanker with the target vehicle. Finally, depending upon the refueling technique utilized, it could also include considerable extravehicular-activities (EVA) on the part of the astronauts. It is generally recognized that the selection of a particular transfer system is highly mission dependent (Gangadharan, 2004).

Orbital propellant transfer depends on three major parameters which influence the type of transfer mode. These are as follows:

I. Total amount of propellant needs to be transferred

II. Total time taken to transfer the propellant

III. Type and properties of the propellant to be transferred

Apart from the above mentioned parameters transfer rate, volumes, pressure requirements, gravity effects of the specific propellant also need to be considered.

For a redundant system there are plenty of design requirements and operational requirements needed to be considered. Few factors are mentioned below

1) Reliability

2) Weight

3) Cost

4) Safety

5) Development difficulties

6) Launch risk

7) Monitoring the operations

Few of the operational requirements which need to be considered:

1) Altitude

2) Solar radiations and flares

3) Micro meteoroids

4) Debris in the orbit

1.1. Earlier Concepts

There are various conceptual systems developed for propellant transfer that are briefly discussed below along with their disadvantages:

1) Tank replacement method

2) Positive displacement pistons or bladders method

3) Draining by linear acceleration method

4) Gas pressurant method

5) Surface tension screens and dielectrophoresis method

1.1.1. Tank Replacement Method

Tank replacement is a straight forward method. It is used to transfer any quantity of propellant from a small to a large tank. This concept involves removal of the empty tank from the spacecraft and replacing it with a new tank from the supply vehicle. It uses Quick-disconnect couplings which would be utilized to minimize EVA on the part of the astronauts. While this concept looks feasible, it has some disadvantages. It is very expensive to carry out, and requires the supply vehicle to carry a heavy payload which in turn requires designing of a bigger launch vehicle (Boretz 1970).

1.1.2. Positive Displacement Pistons and Bladders

The Positive Displacement using pistons and bladders for transfer has a definite advantage in micro gravity conditions. This method incorporates a bladder or piston in the supply tank which pushes the propellant from the supply tank to the receiver tank through the transfer line. This eliminates the problem of ullage control and liquid vapor separation. The time taken to transfer the fuel depends on the design of the bladder or

piston, and its operation. Short comings of this design include the limited life cycle of the

bladder and its inability to withstand temperature higher than those of cryogens such as

liquid hydrogen and liquid nitrogen. Also, the current bladder manufacturing technology

is not sophisticated enough to design a bladder of size more than 50 inches in diameter.

Due to the temperature limitations, bladder life and size its operation is limited to non-

cryogenic applications (Boretz 1970).
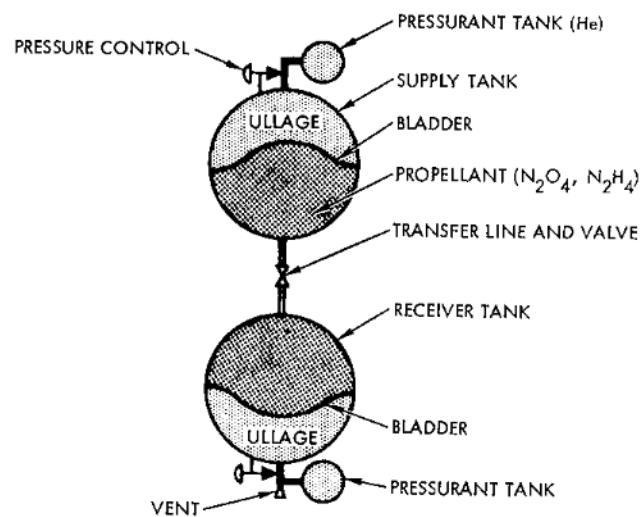
Figure 1 Positive Displacement by Bladder (Boretz 1970)

1.1.3. Draining by Linear Acceleration

Draining by linear acceleration system is for transferring liquid cryogens such as

liquid nitrogen and liquid oxygen. This is accomplished by connecting the receiver tank

below the supply tank, and giving thrust or linear acceleration at the receiver tank. This

makes the system to suddenly move at a velocity and cause the propellant from the

supply tank to flow in to the receiver tank. The magnitude of the acceleration should be

calculated for the required transfer amount. Fluid momentum changes can be avoided by

using fuel slosh dampening system. However, this transfer system is limited by the flow rates possible. From the test study, it was found that using 1-foot diameter of transfer line in an acceleration field of 10^{-4}g will generate a flow rate of 8lbs/sec. An average of 1.5 hours will take to fill a tank size similar to Saturn S-IVB rocket. If the gravity condition is reduced to 10^{-6}g, the flow rate will only be reduced and it will take more than 15 hours. (Boretz 1970).
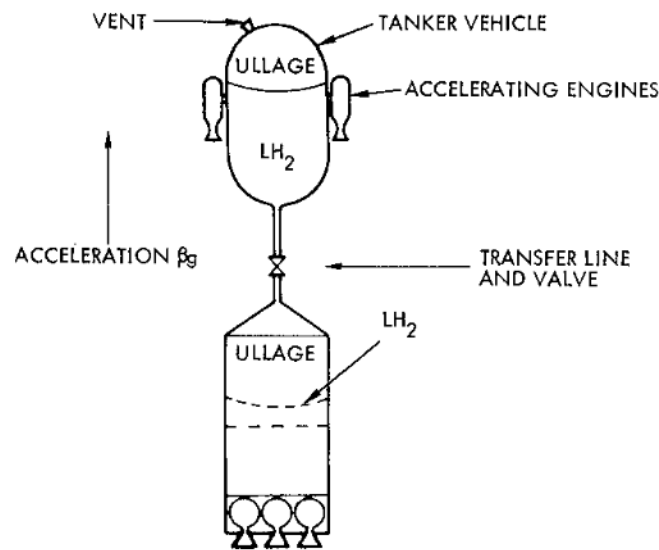
Figure 2 Draining by Linear Acceleration (Boretz 1970)

1.1.4. Gas Pressurant Transfer

For faster transfer of large quantities of liquid cryogenic propellant, gas pressurant system concepts has been developed. Many different concepts have been considered for this type of transfer (Boretz 1970). Which include:

Inert Gas Pressurant

Inert gases are used to increase the gas specific volume by heat. They require low

acceleration level to control the ullage in the tanker. Ans are used to settle the propellant in the receiver tank.

Gas Pressurant System

This method is carried out by using combustion to generate gas for pressurizing the supplier tank, and this pressure is used to transfer the propellant. The exhaust gas needs to be cooled down before they can be fed into the system. This method requires additional cooling technique.

1.2. Transfer Process Considerations

For any type of transfer technique there are many factor that need to be taken into account (Boretz 1970). While they vary by the type of propellant; some common factors are:

1) Gravity Level Requirement

2) Liquid-Vapor Interface during Draining and Vapor Ingestion

3) Gas Pressurant Mass Determination

4) Transfer Line Cooling

5) Tank Thermodynamics

6) Dynamic Consideration Associated with Orbital Propellant Transfer

7) Low Gravity Venting

8) Propellant Settling in Receiver Tank

9) Fuel Slosh Dampening

Each of the above factor is discussed below:

1.2.1. Gravity Level Requirement

The problem of liquid-vapor interface stability is of primary importance in propellant settling, supply tank drainage, and receiver tank filling. It is critical to be able to predict the position and behavior of the phase boundary as a function of acceleration level, tank geometry, fill and drain rates and the physical properties of the fluid being transferred. The acceleration is assumed large enough so that the vapor-liquid interface is originally perpendicular to tank axis. Under these conditions the dispersion law for small oscillations of the interface is easily obtained. Use is made of the fact that small oscillatory flow is always a potential flow and that the fluid velocity is derivable from a velocity potential.

1.2.2. Liquid-Vapor Interface During Draining and Vapor Ingestion

When the tank is draining or filling, a more complex phenomenon ensues. In general, one can assume that gravity level sufficient for settling is also sufficient for interface stability during draining since the motion of the liquid is away from the interface, tending to effectively increase the stability. Higher gravity level would be required for settling since the momentum of the liquid is towards the interface. It is found that the behavior of the draining process is characterized primarily by the ratio of inertia to surface tension forces.

1.2.3. Gas Pressurant Mass Determination

The mass of the pressurant gas required to transfer a given quantity of cryogenic propellant is determined by the following factors. Specific heat at constant pressure, saturation temperature of cryogen corresponding to pressure, total heat transferred to

walls of gas phase enclosure during the time of transfer.

1.2.4. Transfer Line Cooling

While transferring the liquid cryogens, the most important issue is cooling the transfer line. The initial transfer will result in a transient flow which results in the chill down of transfer line. There will be formation of cryogen vapor in the cooling of the transfer lines which leads to large pressure and slug flow and to the expulsion of large quantities of vapor in the receiver tank. This oscillation will disturb the conditions in the supply tank. The duration of the transient period depends on the thermal mass of the transient line and its initial temperature and the rate of ambient heat addition to the transfer line. This process might take up to 3 - 5min.

1.2.5. Tank Thermodynamics

The receiver tank thermodynamics problem arises when cryogenic propellant is loaded into warm tank. Large quantities of vapor will be released as the tank is cooled by the propellant. The dispositions of this vapor is an important consideration in the overall design of the system. Indiscriminate venting will result in uncontrolled acceleration and could be hazardous. Tank wall temperature is generally measured at the beginning by calculating effects of solar radiation, earths albedo and radiation (Boretz 1970).

1.2.6. Dynamic Consideration Associated with Orbital Propellant Transfer

Kinetic energy imparted to the liquid, will exert pressure on the tank walls during the transfer of the propellant from one tank to another. This reaction will impact a change in force in both receiver and supply tank. If there is no dampening system available, this

could result in dynamic instability of the system.

1.2.7. Low Gravity Venting

During the initial transfer process, the liquid cryogen is transferred into an initially warm tank resulting in evolution of large quantities of vapor. To prevent this, low gravity venting is required. This is done by transferring the two-phase fluid ("liquid/vapor") into a vent line inside the receiver tank. It continues to a throttle valve to a state of lower pressure and temperature. The fluid is then passed through a heat exchanger, where the required heat of vaporization is obtained from an external source such as space vehicle waste heat. It is ascertained that only vapor is vented (Boretz 1970).

1.2.8. Propellant Settling in Receiver Tank

In most transfer conditions, linear acceleration will be present for the purpose of ullage control in the supply tank and reduction of vapor ingestion at the supply tank outlet. This may or may not be sufficient for the settling of the propellants in the receiver tank without baffles or other ullage control devices. Minimum gravitational level consideration is required for the propellant in the receiver tank to settle without any external source, thus reducing complexity.

1.2.9. Fuel Slosh Dampening

To control the motion of the propellant inside both supply and the receiver tanks, anti-slosh baffles are used to reduce the sloshing effects. There are many slosh dampening techniques to prevent fuel sloshing. This also helps to diffuse the incoming gas from the supply tank and to prevent ingestion of vapor during the drain process

(Boretz 1970).

1.3. Two-Tank Design Concept

The two-tank design consists of three main modules to improve the storage volume and efficiency. These modules include:

  I.   Centaur module

 II.   Mission module

III.   Liquid hydrogen storage module
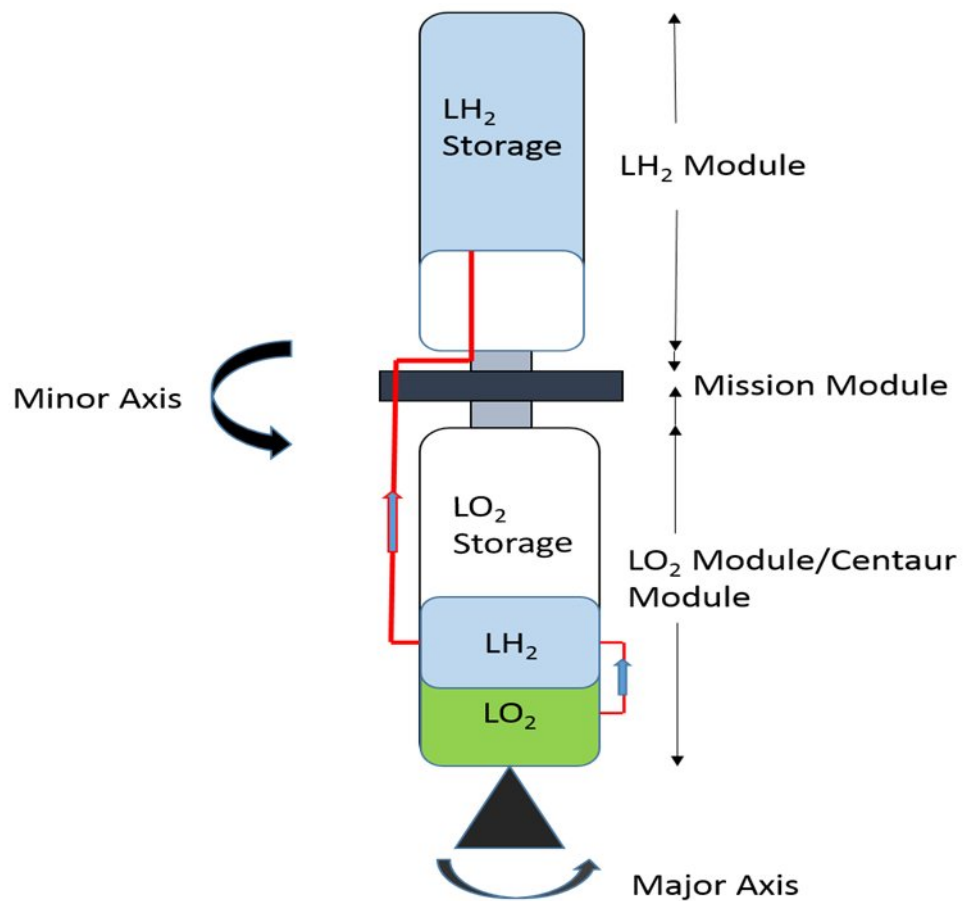
Figure 3 Two-Tank Rotational Settling

The system initially will be a liquid rocket tank (Figure 4). It can vary in size according to the space mission. A t the time of launch the liquid oxygen and liquid hydrogen section of the tank will be filled to the maximum capacity. Solid booster can be used if the mission requires heavy payload. The propellant being stored in the Centaur module will be burned according to the mission requirement. However, the tanks can be designed to have at least 50% of propellant left in the system.

After the system reaches low earth orbit (LEO), it will be placed into a transfer spin. This generates a centrifugal force in the system pushing the propellant out into the outer poles of the fuel tank. Fuel management hardware is located at the outer poles of the fuel tank which controls the propellant flow. This type of new settling approach requires minimum additional propellant expulsion. This system also operates in a very energetically stable state, allowing the excess energy from the system to correct any instabilities experienced from internal or external perturbations. After the system stabilizes at a particular angular velocity, the transfer process of propellant begins by means of helium or oxygen pressurant. There are four major transfers taking place which are discussed below (Gangadharan 2004).
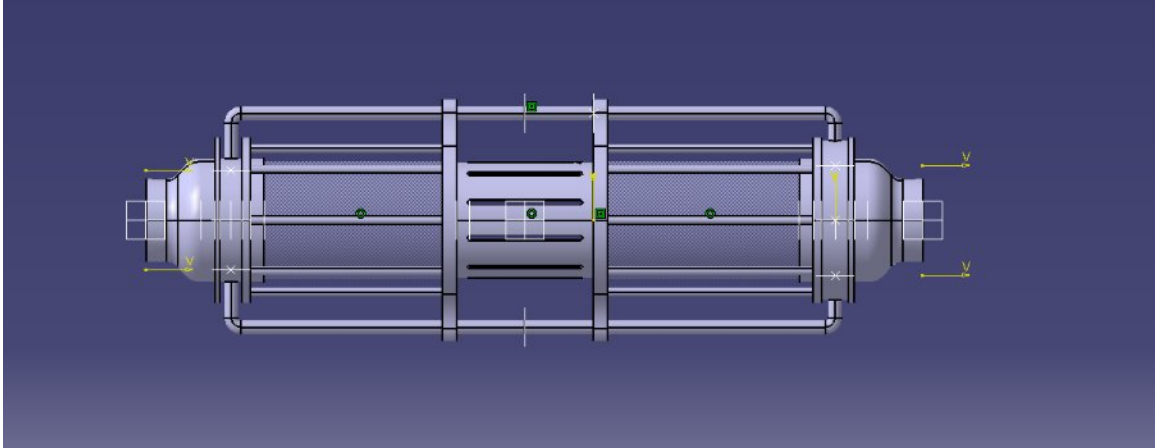
Figure 4 CATIA Model of the System

1.3.1. Transfer Stage One

This process is takes place to cryogenically cool the upper liquid hydrogen storage module and transfers a small amount of liquid hydrogen to the upper storage module from the centaur module. This allows the vacuum to vent from the storage module.

1.3.2. Transfer Stage Two

In this process the remaining liquid hydrogen from the centaur module is transferred to the upper storage module after the upper storage module is sufficiently cooled. After the transfer has taken place the remaining gaseous hydrogen is vented into space to prepare the tank to receive liquid oxygen.

1.3.3. Transfer Stage Three

This process is taking place to transfer all the remaining liquid oxygen from the centaur module liquid oxygen tank is transferred to the liquid hydrogen tank in the centaur module. After these transfer the system is placed at set trajectory on-orbit and

await rendezvous with the subsequent mission elements.

1.3.4. Transfer Stage Four

This is the transfer process where all the remaining propellant is transferred from storage module to the docked space craft.

2. Static and Dynamic Stability of the System

2.1. Torque-Free Motion

Gravity is the only force acting on the system when it is in orbit (If secondary drag force and the gravitational influence of the system other than the planet being orbited is neglected). For this system, the gravitational force is concentrated at the center of mass G. Since the net moment about the center of mass is zero, the system is "torque-free".

$$? ? ?_? ? ? ?_? ? ?$$

$$? ? ? ?? ?? ? ? ? ??$$

L= angular momentum

Z, L, ω, P

Y

X
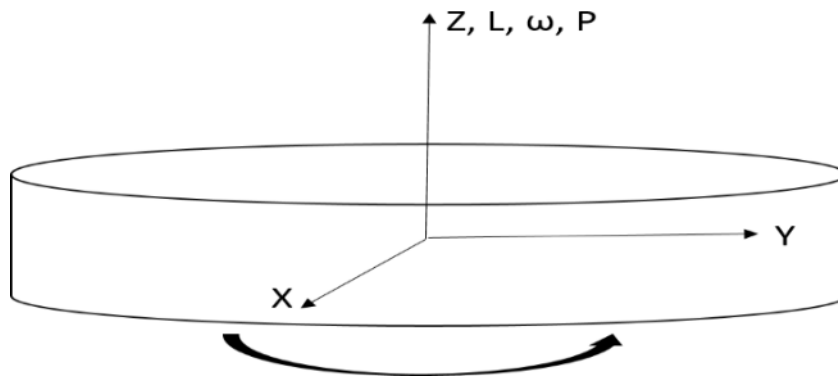
Figure 5 Torque Free Rotation

2.2. Stability of the System

The stability of the system is determined by Euler's Equation

$$? \dot{\omega} ? ?? \quad \overline{??\omega_?\omega_?} ? ?$$

$$? \dot{\omega} ? ?? \quad \overline{??\omega_?\omega_?} ? ?$$

$$? \dot{\omega} ? ?? \quad \overline{??\omega_?\omega_?} ? ?$$

Where A, B, C are the principal moments of inertia, about the x, y, z axis respectively.

If C > A and C > B or C < A and C < B, means that the spin axis is either major or minor axis of inertia. The system will be instable only when it is spinning around the intermediate axis.

If the body is spinning about major axis it is called OBLATE spinner and it is indefinitely stable. If the system is spinning about the minor axis, it is called PROLATE spinner, and is stable with respect to small disturbance.
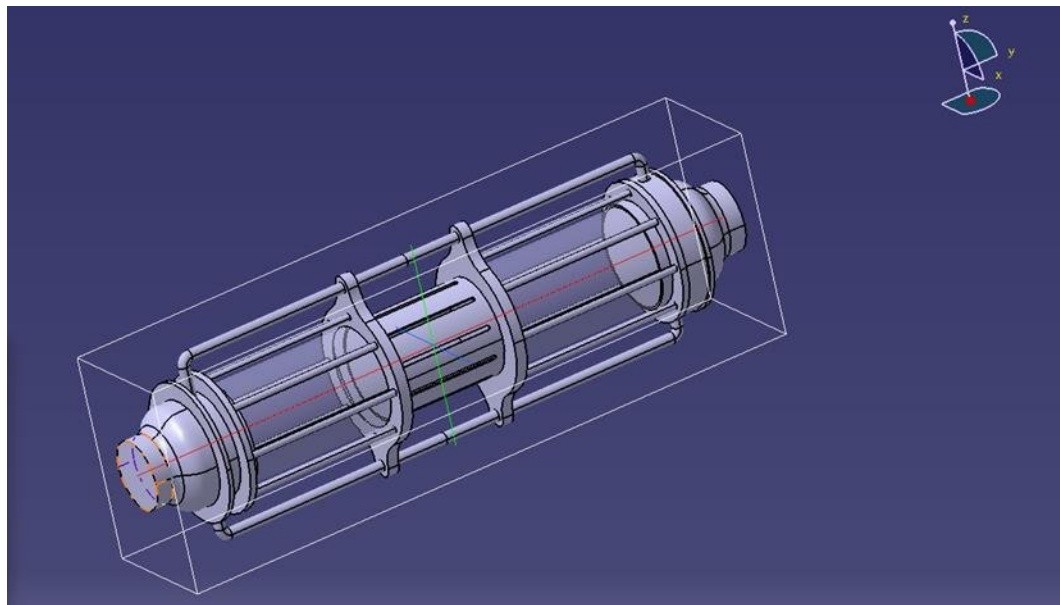
Figure 6 CG of the System

Above is the 3D CAD design of the two-tank design (Figure 6). In this design, the center of mass almost lies at same point as the center of gravity. From the screen shot of the values of inertia it can be observed that $?_{??}\,?^?_{??}\,?^?_{??}$ are very small. Similarly, the values of A and C are same and considered to be along minor axis (Figure 7).

In this case, it is very clear that if the system is spun about the Y axis it will be more stable but the centrifugal forces cannot be achieved at the tank ends. Spinning around the minor axis (that is either X or Z) the system will still be stable though with some small disturbances.
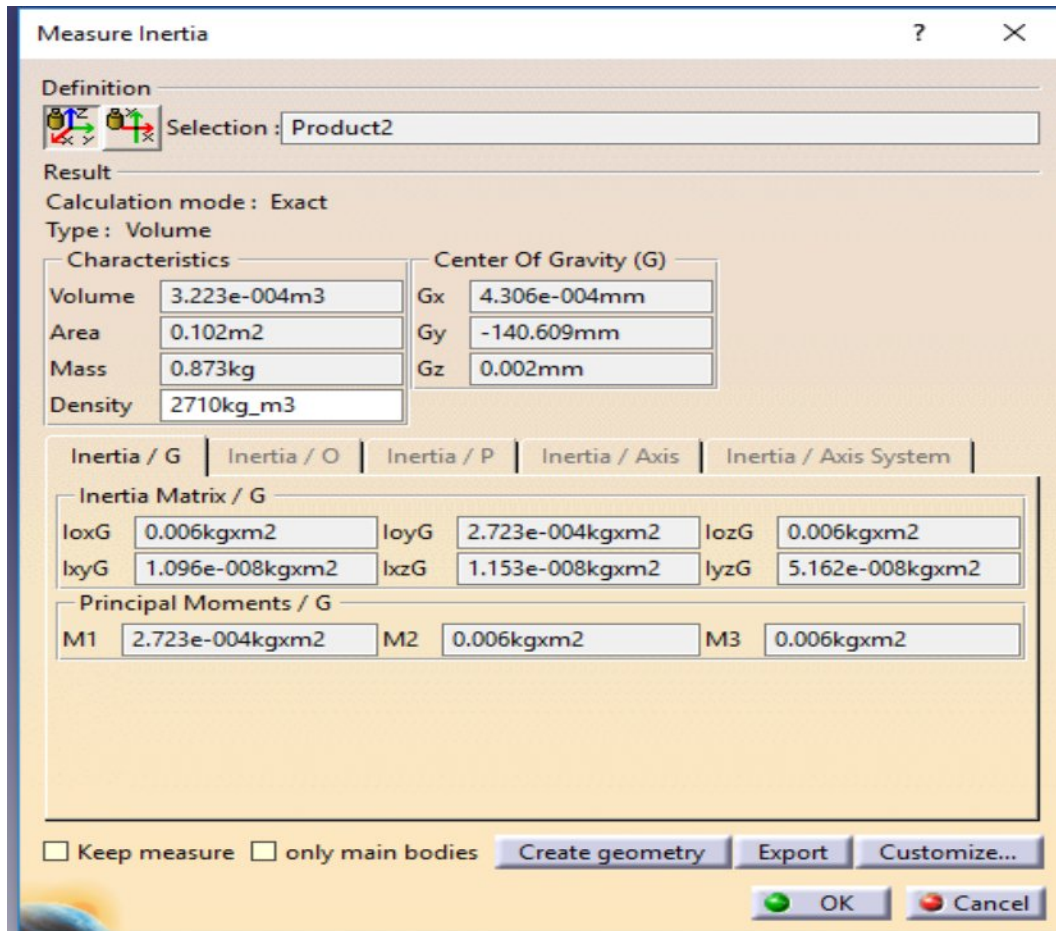
Figure 7 Moment of Inertia values

For this system, the major axis is along the body. So, it can only be spun around the minor axis to achieve the centrifugal force. The rotational kinetic energy will be more if the system is spinning about the minor axis.

$$?_? \; ? \quad \frac{?}{? \; ? \; ?????? \; ? \; ??????} \; ?_?{}^?$$

In an ideal condition where there is no propellant inside and the masses are equally distributed on either side, the system will undergo pure rotation. But since this system has different masses at both sides from the center, at any given point of time it is technically unstable.

To keep the center of mass and the center of gravity of the system at the same point, during the propellant transfer a counter weight system needs to be developed. This counter weight movement is directly proportional to the rate of transfer. The rate of transfer is determines the shift in center of mass.
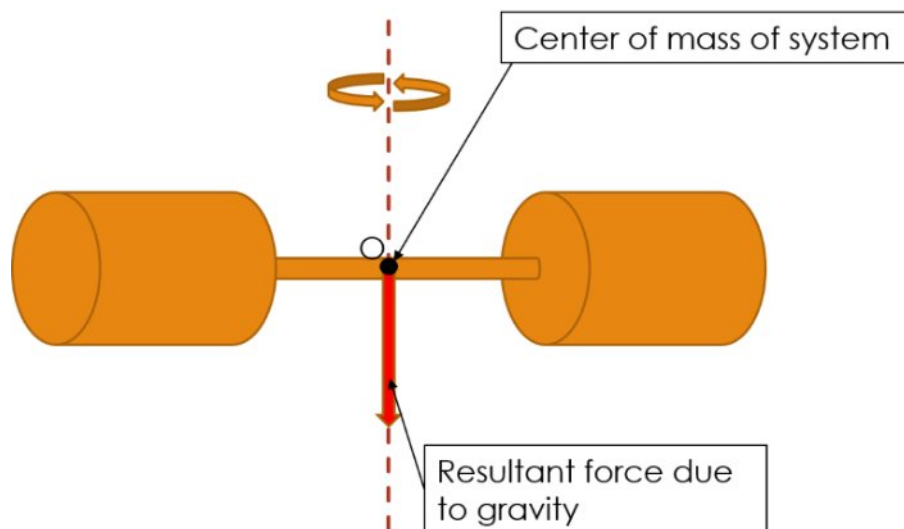
Figure 8 Static Stability of the System

2.3. Center of Mass

2.3.1. Base Equation:

$$? ? \frac{\int ???}{\int ??}$$

Since the motor will only spin the tanks along the minor axis (z-axis), the motion of the

tanks can be assumed to be 2-D along the xy-plane.

2.3.2. 2-D Assumption

Center of mass, can be ignored since any shift in this direction will not add any force. The tanks and connecting rods can be assumed as rigid bodies simplifying the integrations. The liquid inside the tanks can also be assumed as rigid bodies after the rotation has settled the fluid to the extremities.

The calculations for the center of mass of the empty tank system can be combined into one equation using a constant measured value calculated using a model in a CAD program or a simplified center of mass equation for system of rigid bodies. The constant CAD value would be more accurate. We consider the tank to be solid for calculation purpose.

$$?_{??\,????} = \frac{?_{\,?????}\,??_? * \frac{?_{?????}}{?} + ?_{\,?????}\,??_? * \frac{?_{?????}}{?} + ?_{\,?????????} * \frac{?_{????????}}{?}}{?_{\,?????} + ?_{\,?????} + ?_{\,????????}}$$
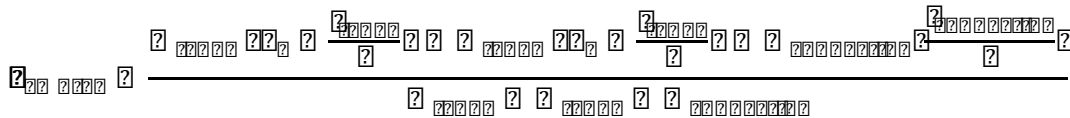
The calculation of the center of mass of the fluid can be calculated using the equation to find the center of mass of a cylinder with constant density:

$$?_{?????} = ?_{?????????} * \frac{? \cdot h}{?}$$

Since the mass and height of the cylinder of fluid changes, the equation for the center of mass of the fluid is:

$$?_{?????} = \frac{??_{\,???} * \overline{?_{\,???????}} ???? * ?_{????} * \frac{\overline{??}_{\,???} * \overline{?_{\,???????}}??}{? * \rho_{???} * \pi * ?_{????}^?}}{??_{\,???} * \overline{?_{\,???????}}??}$$

Where:

- $?_{\,????}$ is the initial mass of fluid in the tank

- $?_{???????}$ is the transfer rate of the fluid between the two tanks

- $?$ is time elapsed

- $?$ is distance of the tank from point center

- $?_{????}$ is length of the tank

- $?_{????}$ is density of the fluid inside of the tank

- $?_{????}$ is the radius of the tank

The center of mass of these two cylinders of fluid will be shifting throughout the fluid transfer and is dependent solely on the quantity of fluid in the tanks.

Once the mass gauging system being developed can provide real time values of mass inside the tank, the expression $??_{??} \overline{?}_{???????}??$ can be replaced with the value of mass which is given out by this system.

Equation 1

The final equation for the center of mass of the tank-fluid system is:

The center of mass will be located at a distance zero from point o when this equation equals to 0. Which makes the equation look like:

$$? ? ?_{????} ??_? \frac{\overline{?}_{????}}{?} ? ? ?_{????} ??_? ? \frac{?_{????}}{?} ? ? ?_{???????} ?\frac{?_{????????}}{?}?$$

$$? ??_{???} \overline{?}_{???????}??\,?? \overline{?}_{????}?? \frac{?? \,??_? \overline{?}_{??????}??}{? * \rho_{???} * \pi * ?^2_{????}}?$$

$$? ??_{???} \overline{?}_{???????}?? ??? ? ?_{????}? \frac{\overline{??} \,??_? \overline{?}_{??????}??}{? * \rho_{???} * \pi * ?^2_{????}}?$$

This equation will not be true except at one instance when the exact amount of fluid is transferred so that the smaller tank has more fluid.

In order to make sure that this center of mass stays at zero at all times, a counter-weight system can be introduced in order to add mass to shift the center of mass.

2.4.   Counter-Weight System

The counter-weight system will consist of a mass attached to a translational system that will allow the mass to move along the systems major axis (Y-axis) (Figure 9).

The counter-weight system will be autonomously controlled using a control code which will shift the position of the mass in order to shift the center of mass back to point o. The code will use the equations discussed before, with the addition of the counter weight center of mass. It will require real time input of the mass in each tank in order to output a real-time position for the mass.
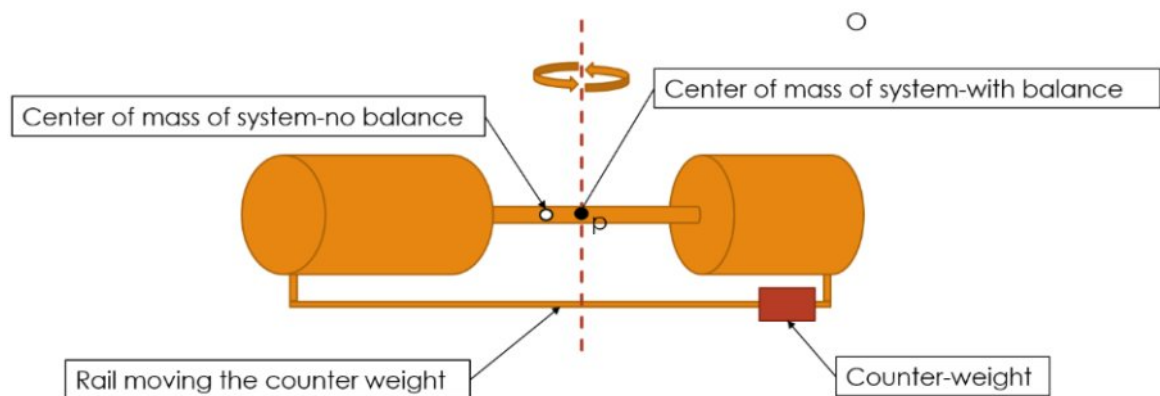

Figure 9 Counter weight system

Equation 1

The final equation for the center of mass of the system is given by:

$$? _? ? \; \frac{? \;_{??} ? \; ? \;_{??} ? \; ? \;_? ? \; ? \;_{??} ? \; ? \;_{??}}{? \;_{??} ? \; ? \;_{??} ? \; ? \;_{????????} ? \; ?? \;_{????} \quad \overline{? \;_{??????}}?? \; ? \; ?? \;_{????} \quad \overline{? \;_{??????}}??}$$

$$? \;_{??} ? \; ? \;_{????} ?? \;_? \quad \frac{\overline{?}\;_{????}}{?}?$$

$$? \;_{??} ? \; ? \;_{????} ?? \;_? ? \; \frac{?\;_{????}}{?}?$$

$$? \;_{??} ? \; ?? \;_{????} \quad \overline{?\;_{??????}}?? \; ??? \quad \overline{?\;_{????}}?? \; \frac{?? \;_{????} \quad \overline{?\;_{??????}}??}{? * \rho_{????} * \pi * ?^2_{?????}}?$$

$$? \;_? ? \; ? \;_{????????} ?\frac{?\;_{????????}}{?}?$$

$$? \;_{??} ? \; ?? \;_{????} \quad \overline{?\;_{??????}}?? \; ??? \; ? \; ?\;_{????}? \; \frac{\overline{??}\;_{????} \quad \overline{?\;_{??????}}??}{? * \rho_{????} * \pi * ?^2_{?????}}?$$

$$? \;_{????} ? \; ? \;_?$$

$$? \;_{????} ? \; ? \;_?$$

Equation 2

The unknowns in this equation are the mass of the counter-weight and the position of the counter-weight assuming the mass of the fluid is known at any time t.

$$? _? \; ? \quad \frac{? _{??} \, ? \, ? _{??} \, ? \, ? _? \, ? \, ? _{??} \, ? \, ? _{??} \, ? \, ? _? \; ??? \; \frac{?}{?}?}{? _{??} \, ? \, ? _{??} \, ? \, ? _{???????m?} \, ? \, ?? _{m?m?} \quad ? _{???????}?? \, ? \, ?? _{m?m?} \quad ? _{???????}?? \, ? \, ? _?}$$

Equation 3

To solve for the minimum mass of the counter-weight needed a simple assumption can be made and the maximum value of the extreme cases can be used. It can be assumed that the mass must have a maximum distance from point o based on the design parameters of the tank system. Using this assumption, the equation can be rewritten and tested for different tank phases to calculate the mass needed to shift the center of mass back to point o.

$$? _? \; ? \quad \frac{? _{??} \, ? \, ? _{??} \, ? \, ? _? \, ? \, ? _{??} \, ? \, ? _{??} \, ? \, ? _? \; ??? \; \frac{?}{?}?}{??? \; \frac{?}{?}?}$$

Equation 4

The last equation is a rewritten form of equation 3 solved for position r of the counter-weight. This equation is the one that will be used in the code controlling the counter-weight system.

$$?? \quad \frac{? _{??} \, ? \, ? _{??} \, ? \, ? _? \, ? \, ? _{??} \, ? \, ? _{??} \, ? \, ? _? \; ??? \; \frac{?}{?}?}{? _?} \quad \frac{?}{?}$$

3. Mass Gauging

Traditional methods of fuel gauging require the presence of an external gravitational field. These methods depend on buoyant forces acting on a surface level indicator, and are mainly used in automobile fuel gauge monitors. These methods will not work when the system is not under influence of gravitational field, since the position and shape is unrelated to the volume of the liquid in the tank.

Fuel volume estimation on spacecraft instead uses an indirect method for fuel gauging, such as equation-of-state estimation, measurement of spacecraft dynamic, and burn time integration.

For the equation-of-state estimation the tank needs to be pressurize initially. The mass is calculated by monitoring the propellant burnt. the volume of the ullage is calculated by taking the pressure and temperature of the remaining ullage in the tank. This method will require additional hardware for the pumps, valves thus making the launch vehicle heavier.

The next method is measuring the spacecraft dynamics. This is done by measuring the spacecraft's dynamic response to acceleration. The total average mass of the spacecraft during the burn is subtracted by the fixed mass of the spacecraft, thus estimating the fuel left in the tanks. The additional propellant are burnt to calculate the mass and is a big disadvantage for this method.

The burn time integration method is a hand calculation method. The thrust firings are recorded and the total propellant usage is estimated through assumptions. This method is inaccurate and provides only approximate value (Fortescue 2003).

3.1. Experimental Modal Analysis

Experimental Modal Analysis (EMA) is a method which uses acoustic forces to test structures. The natural resonance of the test structure is excited by applied force, which can be in the form of point source. The sensors affixed to the structures record the amplitude of the acoustic response across the range of resonating frequencies.

In this experiment the acoustic force applied to the structure is a white-noise function since it gives a discrete impact. A broad-band white-noise is used here. A white noise usually contains spectrum of all frequencies within a specified range with each frequency component having a similar spectrum power. By applying all possible driving frequencies to the tank, it can be ascertained that the full set of structural resonant frequencies is present within the applied signal. Therefore, natural vibrational modes of the structure will be excited. This results in an increased amplitude in sensor response at the excited mode frequencies.

To record and separate the resonant frequency of the tank, two non-invasive sensors are attached to the tank. The first sensor is placed closer to the actuator which provides the input spectrum of the white-noise frequencies. This sensor is referred to as "monitor" as it generally reproduces the input spectrum with very little resonant mode amplification. The second sensor is placed far from the monitor, and produces an output that consists of the attenuated white noise spectrum with the resonant frequencies preferentially excited.

In this EMA method, Fast Fourier Transforms (FFT) of the monitor and sensor signals are computed and the ratio of sensor to monitor FFTs is derived to construct the Frequency Response Function (FRF), the signal FFT is normalized by the monitor FFT

and therefore isolates those frequency components that only appear in the signal sensor. This way, the resonant mode of the tank is isolated and extracted from the applied white noise spectrum. The response function of the tank is calculated using the equation:

$$? \, ?? \, ?? \, \frac{? \, ?? \, ?}{?? \, ?}$$

Modal techniques can therefore be used as real-time diagnostics of structural properties. Fluid loading increases the effective mass of the loaded structure, resulting in a decrease in the structure's resonant frequencies.
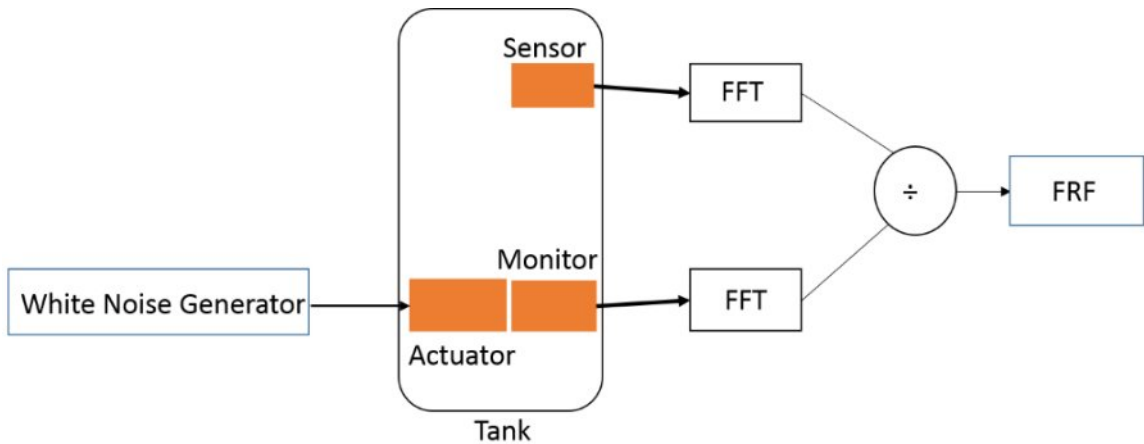
Figure 10 Sensor Placement

4. Experiment Setup

4.1. Ground Test Bed Setup at ERAU

The ground test bed setup at ERAU is an experimental setup consisting of a stepper motor which drives the center shaft through a reduction gear mechanism (Figure 11). MATLAB code is programmed to control the motor and also inputs such as rpm and rate of slow down. GOODYEAR air balloon suspension is used for the prevention of vibration. The maximum speed this set up can take is 400rpm, and this restriction is purely due the design of the test bed.
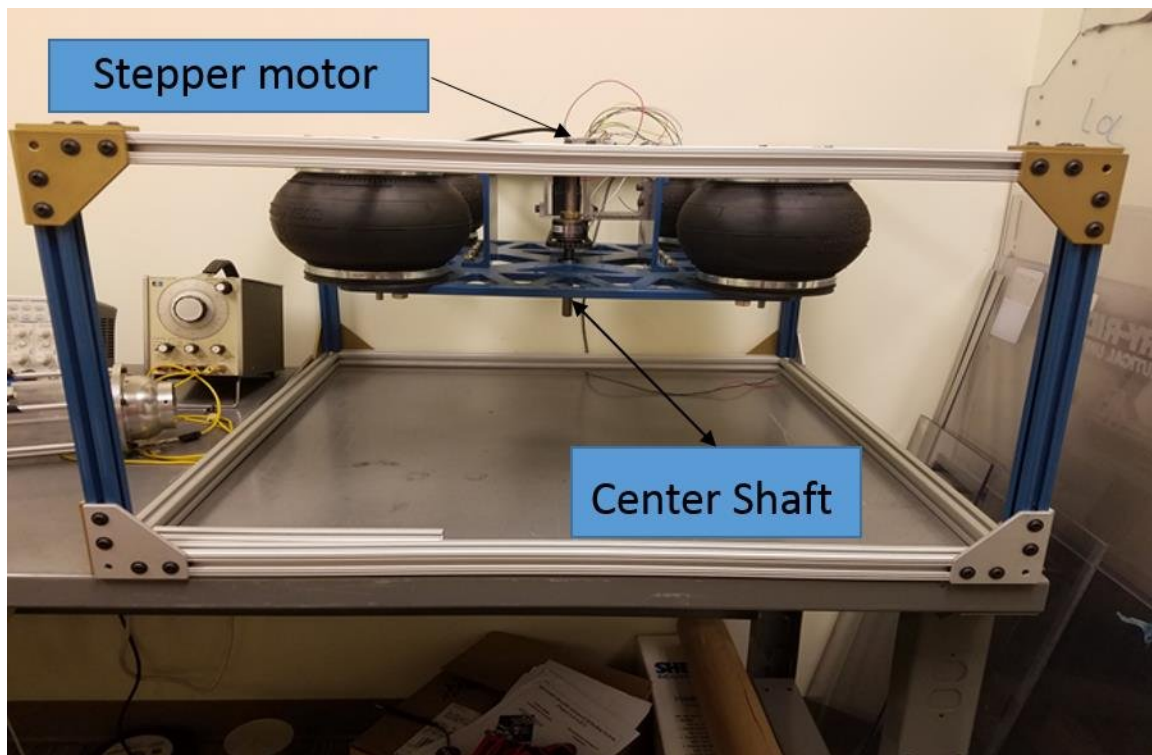
Figure 11 Test bed

4.2.   Prototype Build

The prototype is constructed with reference to the actual system. This consists of two cylindrical tank of identical size. The tank is 5cm in radius, 25cm in length, enclosed by a semi sphered aluminum cap which is also 5cm in radius. The two tanks are connected by an aluminum housing which accommodates the battery pack. The aluminum housing also supports the frame for data acquisition devices. The system houses a transfer line, which is 10mm in diameter. These tanks hold water during the experiment and have inlet hole of 1cm diameter for filling and draining the liquid. Outside the tank PZT (lead zirconate titanate) sensors are fixed along the sides of the tank.

4.3.   Sensor Subsystem

The sensors and the actuator are PZT (lead zirconate titanate) transducers which are fixed to the tank using a thin double-side adhesive (Figure 12). The actuator is driven by a white noise generator and provides a broad band excitation signal to the experimental tank. The signal is amplified by a compact piezo driver that sets up the TTL signal from the white noise generator to a proportional signal with an RMS voltage of ±200V. The sensors produced a voltage signal at the rate of 100s mV, which is converted from the mechanical vibrations produce in the tank.
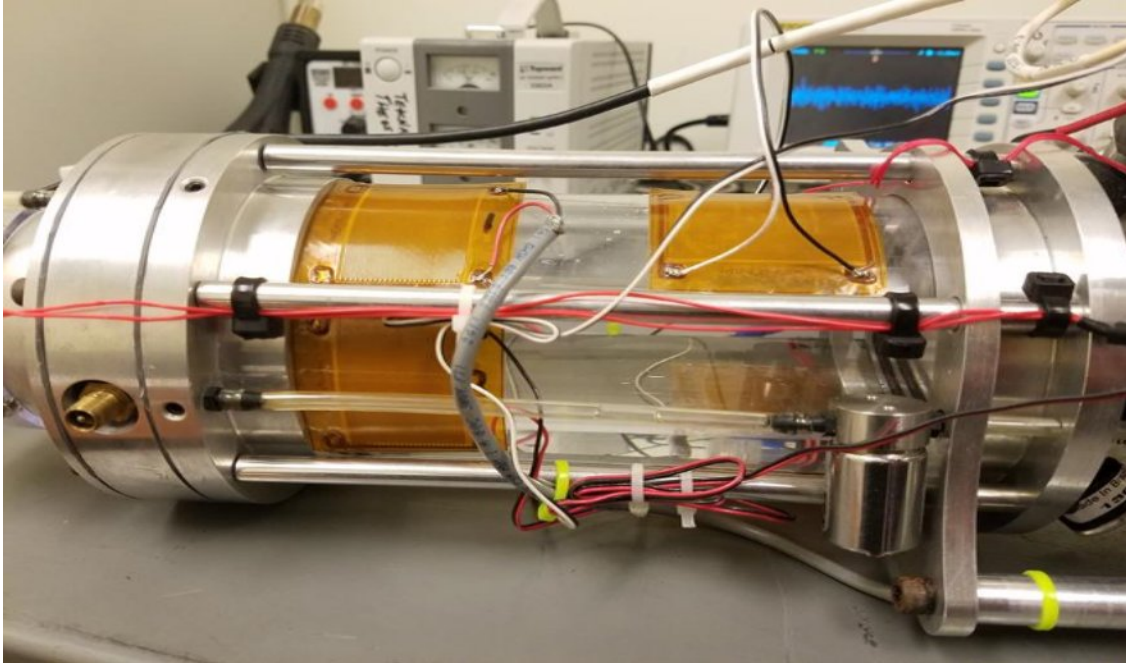
Figure 12 Sensor Placement

4.4. Electronic Subsystems

The electronic subsystems are the devices which send a pre-recorded white noise signal to the actuator. The signals from the sensors and monitor are stored on a memory card. The subsystems also control the timer for the pump and solenoid valve. For the static test, when the device is placed on the table without mounting on the spinning rig the power is supplied directly (Figure 13). A DC power converter is used for the power supply, and a digital oscilloscope is used for monitoring real time frequency. For dynamic testing the electronics are powered by two Lipo (Lithium-ion Polymer) rechargeable battery packs which produce 12VDC. We use Arduino to generate white noise and frequency for white noise is controlled using voltage controller. The data is collected using a micro controller (Sliceware). The data is then downloaded using the software written by Sliceware. This software gives raw data and FFT is performed using a MATLAB code. The Nyquist frequency lies well above the upper end of the frequency
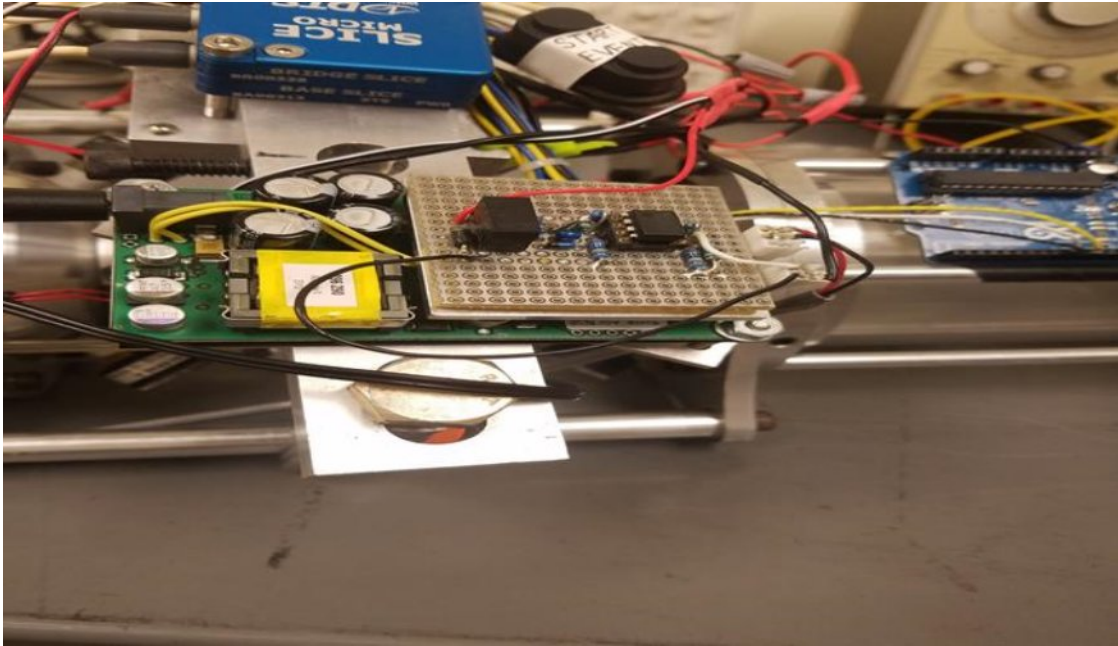
range of interest, 0-5kHz.

Figure 13 White-noise generator

5. Experimental Result

Initially the system is placed on static position for static test. First direct power supply is given using a DC power converter. A constant of 11VDC is given in to the system, which produces a resonant frequency between 2054 – 2081 Hz. The mass in the tank is tested statically by two orientations vertically and horizontally. First, the tank is tested without any liquid and then for each test case 50ml of liquid is added. For each test case the trial is repeated 10 times. Table 1 summarizes the various test cases

Table 1 Test Cases

No of test cases	Horizontal orientation	Vertical orientation
Test case 2	50ml	50ml
Test case 3	100ml	100ml
Test case 4	150ml	150ml
Test case 5	200ml	200ml
Test case 6	250ml	250ml

A screenshot of the graphs (Figure 14) created using a trial run of the empty tank is shown below:
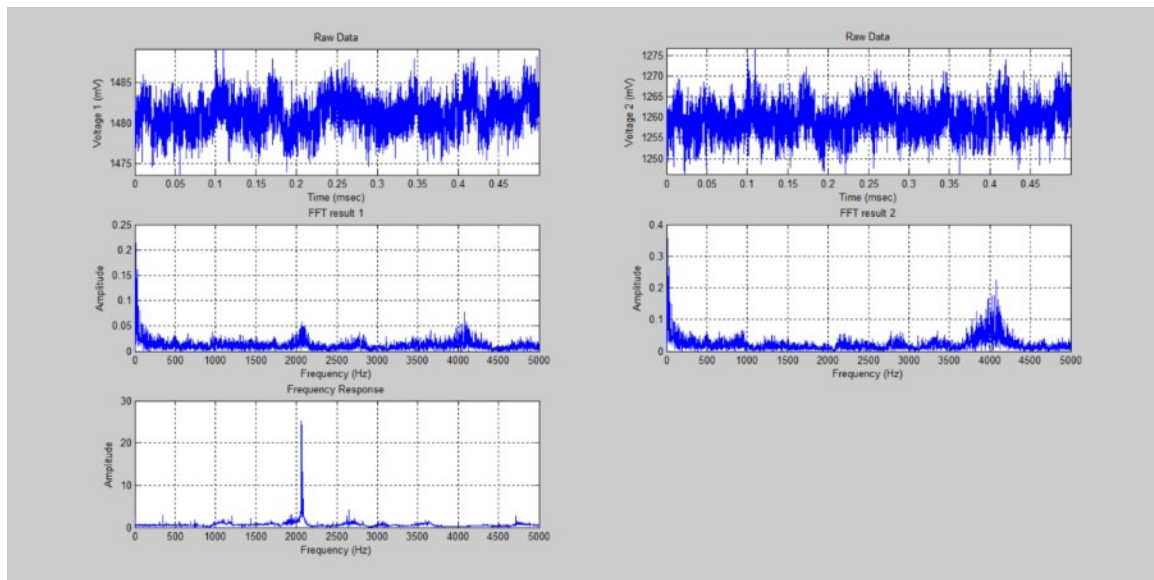
Figure 14 Frequency Response Function Data

Graph 1 and 2 (top right and left) are the sensors output to the data collection system (DTS). This is the raw data collected by the sensors where graph 1 (top left) is the output sensor and graph 2 (top right) is the input sensor. Graphs 3 and 4 (middle left and right) are the Fast-Fourier Transforms of the raw data collected by the sensors. Graph 5 (bottom left) shows the frequency response function of the tank. The below (Table 2) table shows the frequencies for each test case in each trial. There is a substantial decrease in frequency when the fill fraction of the tank is increased. Which means that if there is an addition of mass, the frequency output reduces.

Table 2 Experimental value

Horizontal Orientation				Vertical Orientation			
50ml	100ml	150ml	200ml	50ml	100ml	150ml	200ml
1989.746094	2873.779297	2838.134766	2070.3125	2728.271484	1992.1875	3670.654297	2558.59375
1629.150391	3616.943359	2885.742188	2061.767578	1962.890625	2017.822266	3662.109375	2951.660156
1591.308594	3559.570313	2855.224609	2066.650391	1964.111328	1945.32748	3666.992188	3084.716797
1989.6584	3615.722656	2883.300781	2069.091797	4312.744141	3060.302734	3663.330078	1669.921875
194.0917969	3590.087891	2292.480469	2072.753906	1654.052734	2356.2554	3679.199219	3111.572266
2070.3125	2069.091797	2874.755859	2065.429688	1973.876953	1722.412109	3665.771484	1668.701172
2066.650391	2583.4578	2880.859375	2066.650391	4311.523438	2015.380859	3663.330078	1579.6498
2071.533203	2072.753906	2866.210938	2071.533203	1965.332031	1828.613281	3640.136719	1663.818359
2065.429688	2067.871094	2883.300781	2072.753906	1970.214844	2017.822266	3662.109375	1843.261719
2070.3125	2073.974609	2875.976563	2072.753906	4302.978516	3345.947266	1754.150391	2600.097656

The Frequency Response Functions are recorded across several fill fractions. This fill fraction in this tank is up to 60%. For each test case the 10-trial average is taken, and using MATLAB code, the Fast Fourier Transform (FFT) is performed.

5.1. Test Case 1 (50ml horizontal)

Results from the first test case which is shown in the figure 15, the tank is filled with 50ml of fluid and tested with a horizontal orientation. It can be seen that the highest peak lies from 4000Hz to 45000Hz. Since the fill fraction is only about 20% the Frequency Response Function (FRF) is very high.
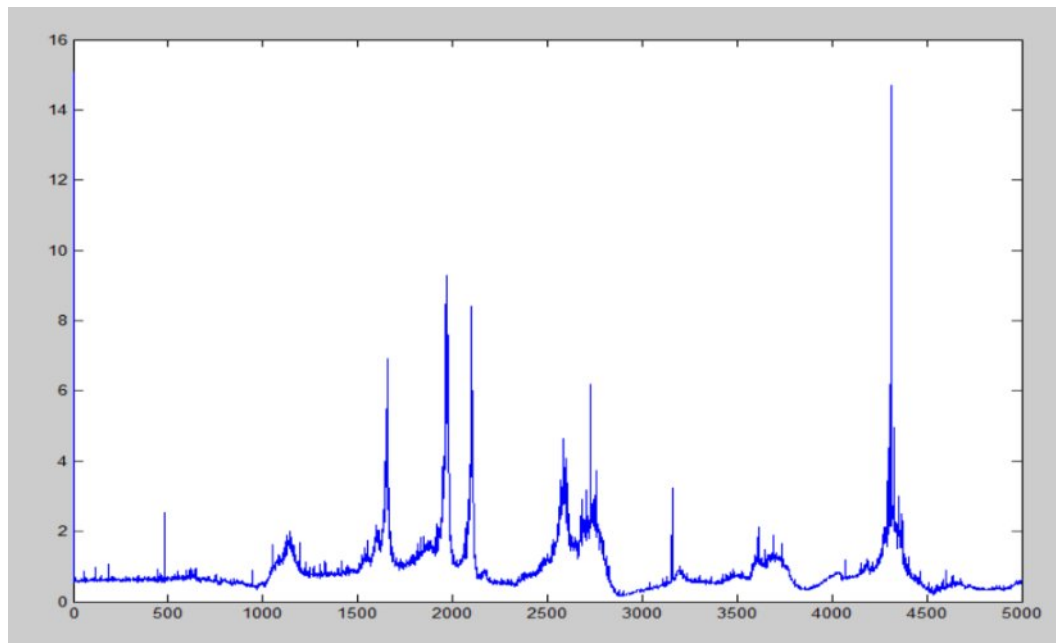

Figure 15 Test result for 50ml horizontal

5.2. Test Case 2 (100ml horizontal)

In the second test case an another 50ml liquid is added to the tank in the same orientation bringing the total volume to 100ml. This increases the fill fraction by 10%. Now for 30% of fill fraction the highest peak on the Frequency Response Function(FRF) lies between 3500Hz to 400Hz (Figure 16), this shows that with addition in mass there is a reduction in FRF.
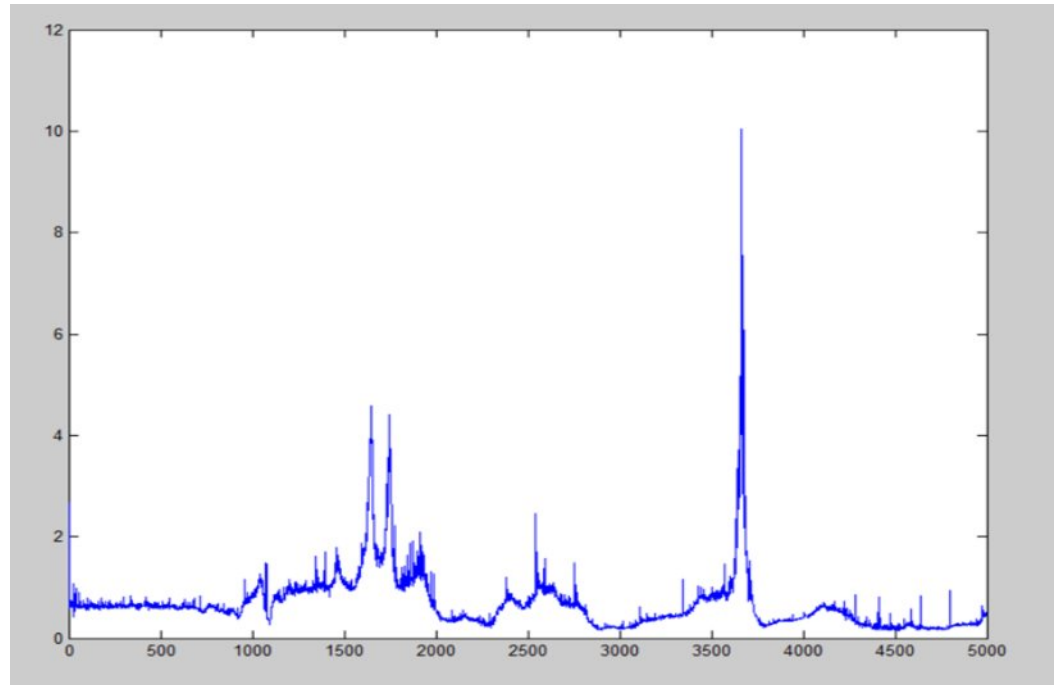
Figure 16 Test result for 100ml horizontal

5.3. Test Cases 3 and 4 (150ml and 200 horizontal)

Test cases 3 and 4 are done in the same orientation adding another 50ml of liquid in each trial. This increases the fill fraction by 10% more bringing it to 40% of fill fraction for test case 3 and 50% for test case 4. The experimental graphs for both test cases (Figure 17 and Figure18) shows that the peaks did not move much due to the liquid fill fractions touching the sensor line. This will be solved once the system is in microgravity conditions where the liquid will be scattered unlike on-earth conditions where the liquid is in constant touch with the sensor. But once the liquid line crosses the sensor line, resonant disturbance will decrease. This it will give the exact result.
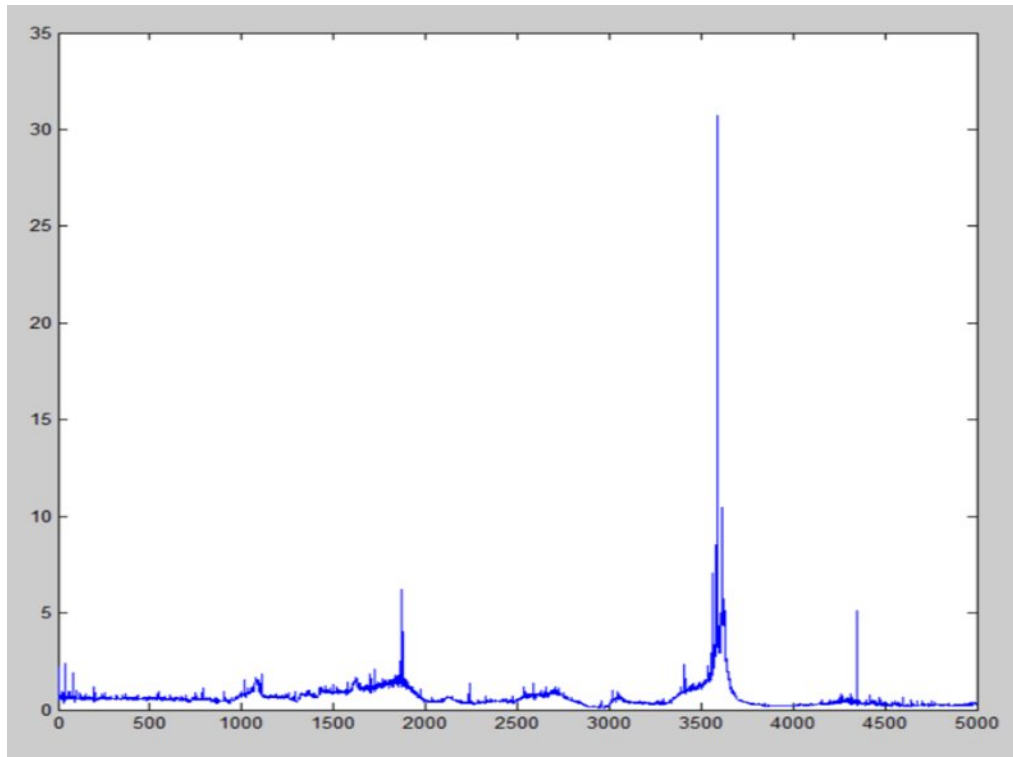
Figure 17 Test Result for 150ml Horizontal
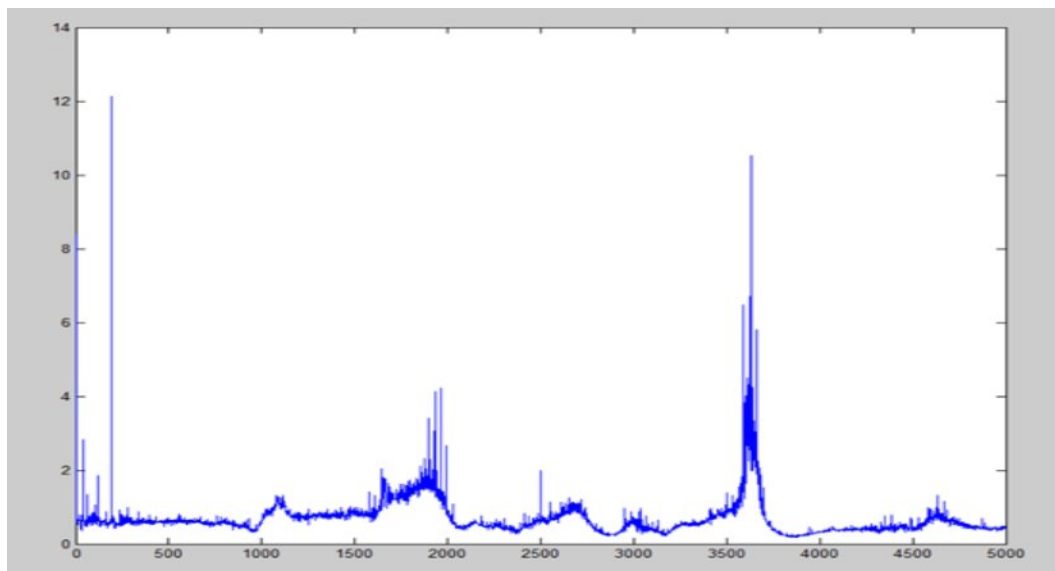
Figure 18 Test Result for 200ml Horizontal

5.4. Test Case 5 (250ml horizontal)

Now for this test case the fill fraction is 60%, for this amount the Frequency Response Function will be less compared to the previous test case 3 and 4. This is because the resonant frequency is not disturbed by the static liquid. From figure 19 it can be seen that the peak of FRF is between 2500Hz and 3000Hz.
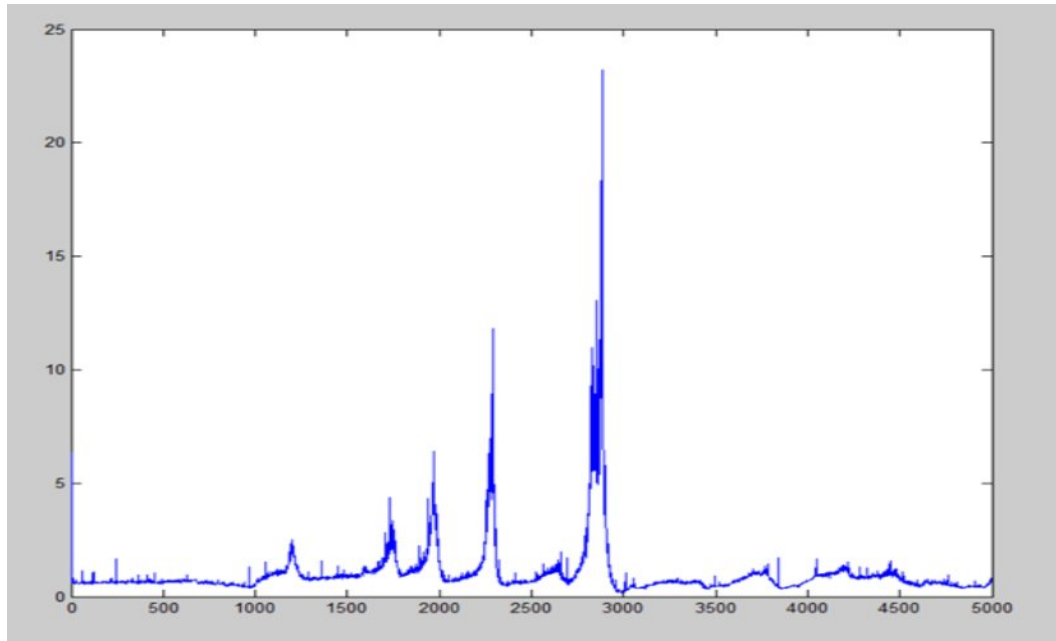

Figure 19 Test Result for 200ml Horizontal

5.5.   Test Cases in Vertical Orientation

Experiments were repeated with the system in vertical position, using the same fill fractions from 20% to 60% with a 10% increment. The results are shown in figures 20 to 24
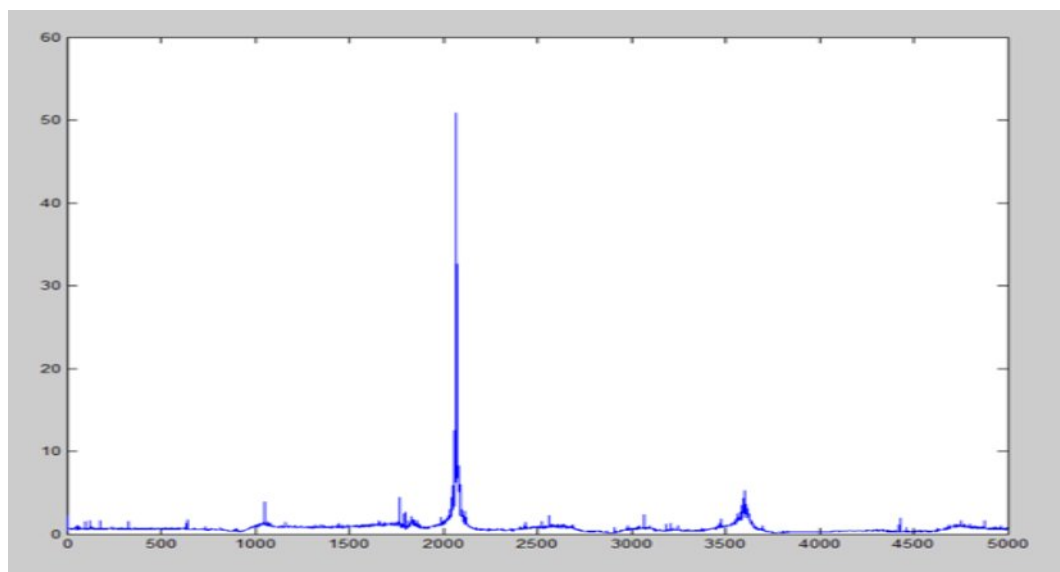
Figure 20 Test result for 50ml vertical
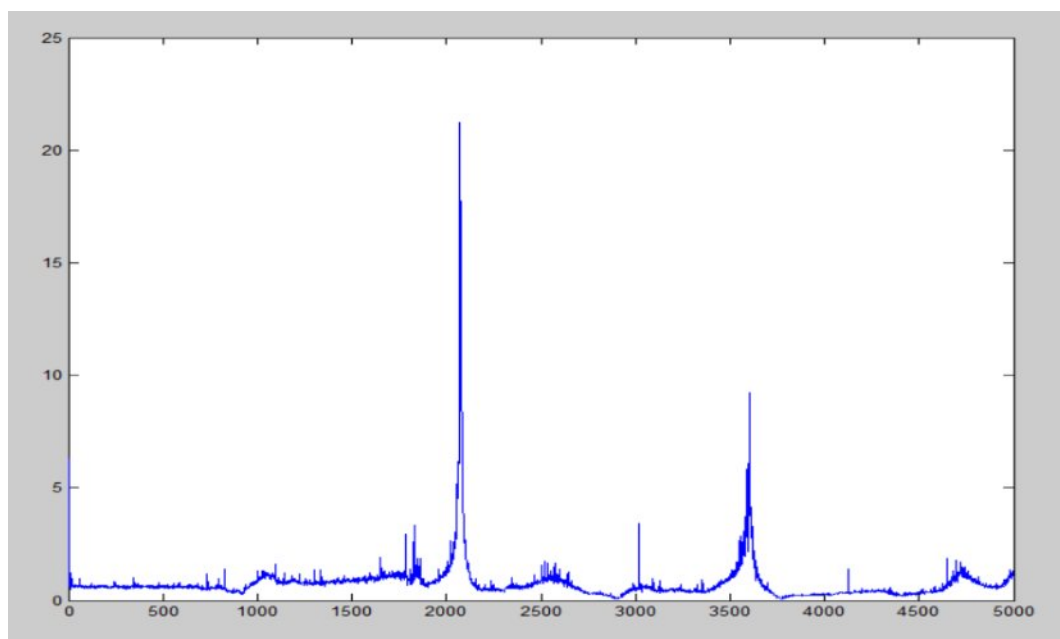
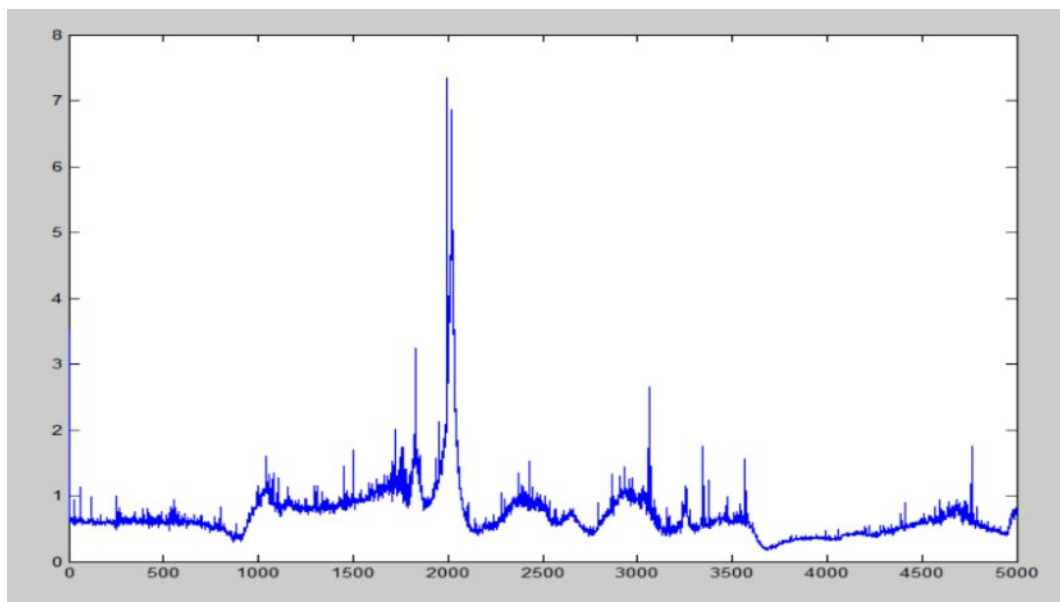Figure 21 Test result for 100ml vertical
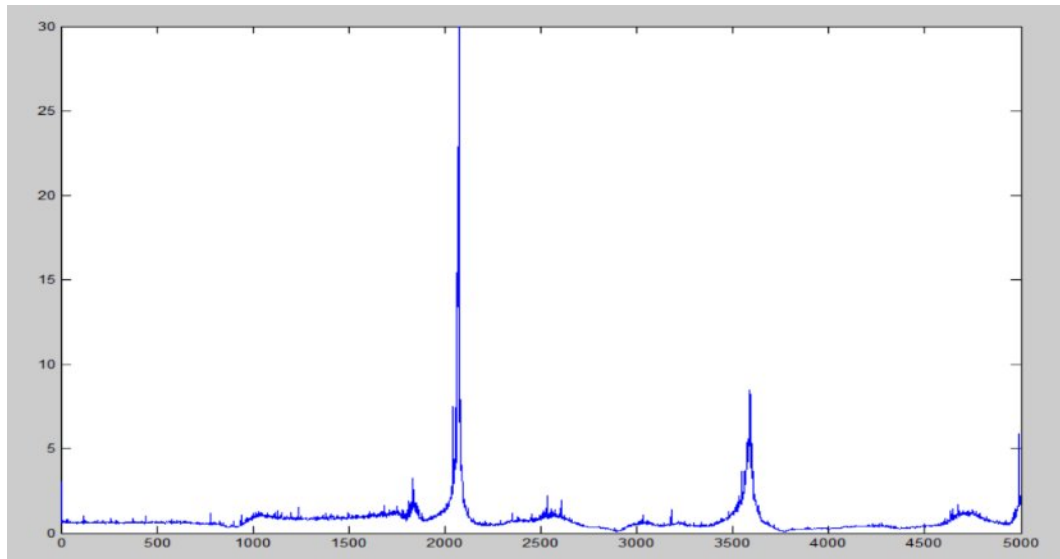
Figure 22 Test result for 150ml vertical
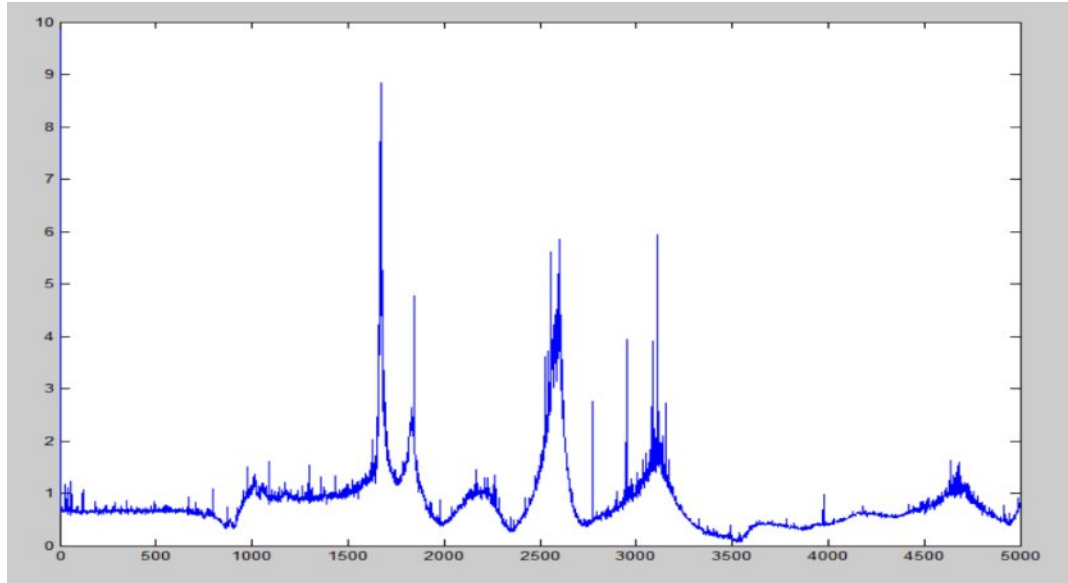

Figure 23 Test result for 200ml vertical

Figure 24 Test result for 250ml vertical

From all these graphs, it can be observed that in the vertical orientation the peaks did not move much because of the sensor placement. The sensor placement when the system is in vertical orientation plays a major role in the output value. Moreover, the prototype setup has only one output sensor connected to the microprocessor. If the sensors are smaller in size and if at least two output sensors are available, more accurate results can be obtained in the vertical orientation. But this system spins around the primary axis thus making it aligned in horizontal position. The vertical orientation experiment is necessary to validate the sensor performance.

6. Computational Approach

Computational approach is taken to observe the system work in-process, thus providing an idea of how the fluid would transfer in real time. In this research the computational approach is split into two phases. The first phase involves performing computational finite element analysis on ANSYS Fluent. The second phase involves computational fluid dynamics where the behavior of System is analyzed under microgravity condition in STARCCM.

6.1. About Computational Fluid Dynamics

The Computational approach resorts to numerical calculation using "Computational Fluid Dynamics" (CFD) software. CFD is an ensemble of numerical methods that allows for finding an approximate solution of a fluid dynamics problem. It involves fluid mechanics equations which are computationally solved.

The solution obtained is not an accurate value but is an approximate one since the Navier-Stokes equations are solved computationally by discretization. Some equation terms are too complex to be solved and are replaced by empirical but inaccurate models. It happens especially in turbulent flow regimes (Paul, 2014).

However, with the advancement of computers since 1950s, powerful graphics and 3D interactive capability, the use of CFD has gone beyond research and into industry as a design tool. Current workstations offer enough computational power to provide very satisfying solutions.

Even if the conditions are ideal when compared to the experiment, the simulation is complementary with the experimental study. Experiments provide macro data at certain points in the flow field, while a numerical simulation provides a detailed resolution such

as turbulence, viscous forces and velocity. These are some of the reasons why CFD is a powerful and necessary tool to resolve complex dynamic and flow problems such as propellant slosh. Finding the solution of a fluid dynamics problem comes down to solving a differential equation. In the case of a Newtonian fluid, the solution of Navier-Stokes equations are employed. The Navier-Stokes equations are a set of partial differential equations describing the processes of heat and mass transfer. The velocity of the fluid is much lower than the speed of sound and air is assumed to have constant density. Assuming air is incompressible and invisid, the Navier-Stokes equations reduced to Euler's equation (where $?$ is the velocity of the fluid particle):

$$\frac{??}{??} ? \overrightarrow{????} ??? ? \quad \frac{2}{?} \overrightarrow{????} ?? ?\Delta?? ? ?$$

These equations have no known general analytical solution (i.e. no Direct Numerical Simulation or DNS), but it can be approached. Thus, it is necessary to resort to the Reynolds- averaged Navier-Stokes equations (RANS), which are a very accurate and precise approach alternative to direct calculus.

$$? ?\frac{??_?}{??} ? \frac{?}{??_?} ??_???? ? \frac{??}{??_?} ? \frac{?}{??_?} ??? \overline{??_???}? ??$$

With v=v̄+v^' written in the temporal mean plus fluctuation decomposition.

Owing to the $??_???_??$ term, a problem in closure appears. This additional term embodying the Reynolds equation, confines and requires the using of a turbulence model. In this case, the K-Epsilon model is used. To solve this problem computationally, the method of finite volume is employed. It relies on a geometrical meshing of the domain (surface and volume) in which the fluid flows. Very pertinent in fluid dynamics as it deals with the classical quantities conservation (momentum, energy, mass), this method

reckons what goes in and what goes out of a mesh (i.e. of a finite volume). The residuals from the simulation calculating the boundary condition along the mesh grids report the difference between the ingoing and outgoing volume in meshes and assesses the accuracy of the simulation. When the residuals grow above a certain value, the calculation is considered as not convergent and the boundary conditions are altered to enable solution convergence.

6.2.   Assumptions in Computational Fluid Dynamics

The CFD domain is an idealistic region where many real-life factors are not accounted for. Few of the assumptions taken into considerations are:

1) Ideal environmental conditions

2) The tanks are made to spin at 14rpm

3) Thickness of the tank wall is neglected

4) The air is pressurized at 10psi

6.3.   Modeling of Tank in ANSYS Fluent

ANSYS Fluent was used to design different tank geometries and simulate the flow in the tanks and connecting lines along the structural response. The flow in the tanks and the connecting lines and the structural response are simulated with ANSYS Fluent. For each geometry, the minimum operating rotational velocity and the structural response have been designed with Ansys in 2D: a rectangular tank, a cylindrical tank with round end caps and a tank with a cylindrical body and square end caps.

All geometries have a tank length of 13cm, and height of 4cm and is symmetrical around the Y-axis. The connecting lines are positioned in the same region for all the setups.
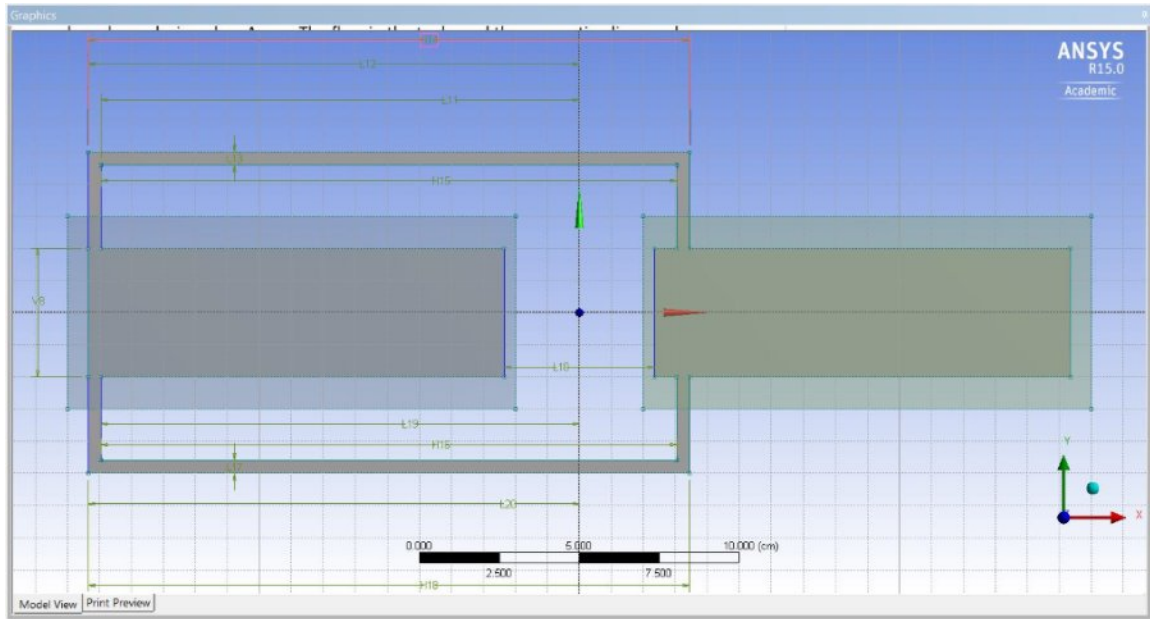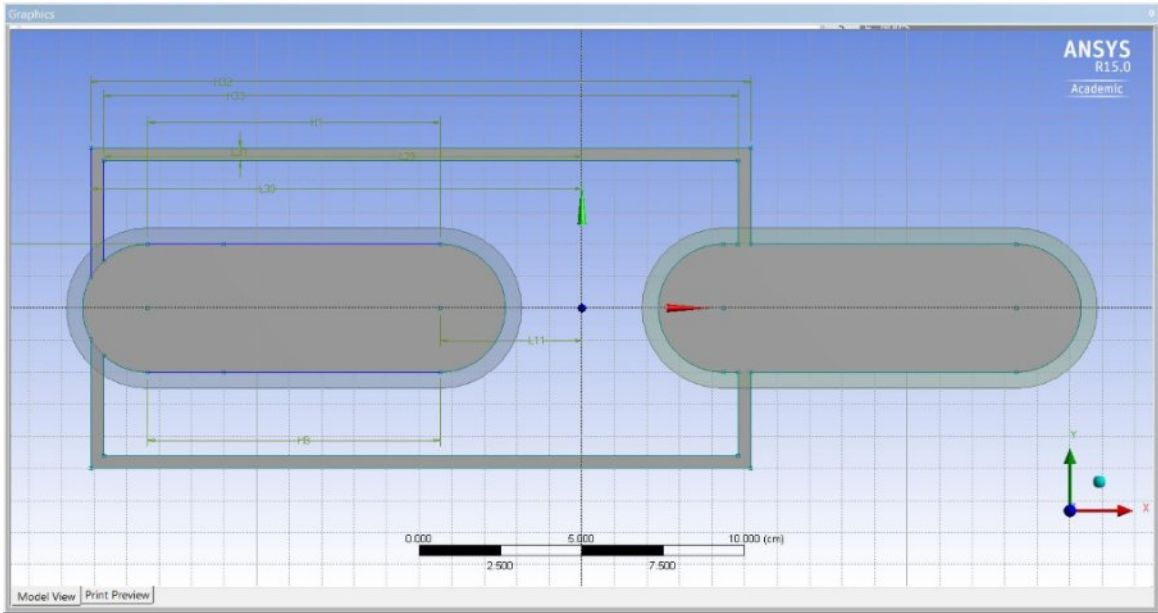

Figure 25 Model design for flat head

Figure 26 Model design for cylindrical head

6.4.   Experimental Layout:

Figure 27 shows the initial setup for the CFD analysis in air volume fractions. Water is filling half of one tank at its edge and there is absolute vacuum in the other tank. Air inside the water tank is pressurized at 10 psi. The whole system is made spin around the Z-axis. The rotation center is the origin of the plane. The pressure force from the air in and the rotation push the water toward the connecting lines. The water will be then being transferred to the other tank. The pressure and the flow are simulated with Ansys. The transfer of the liquid is studied.
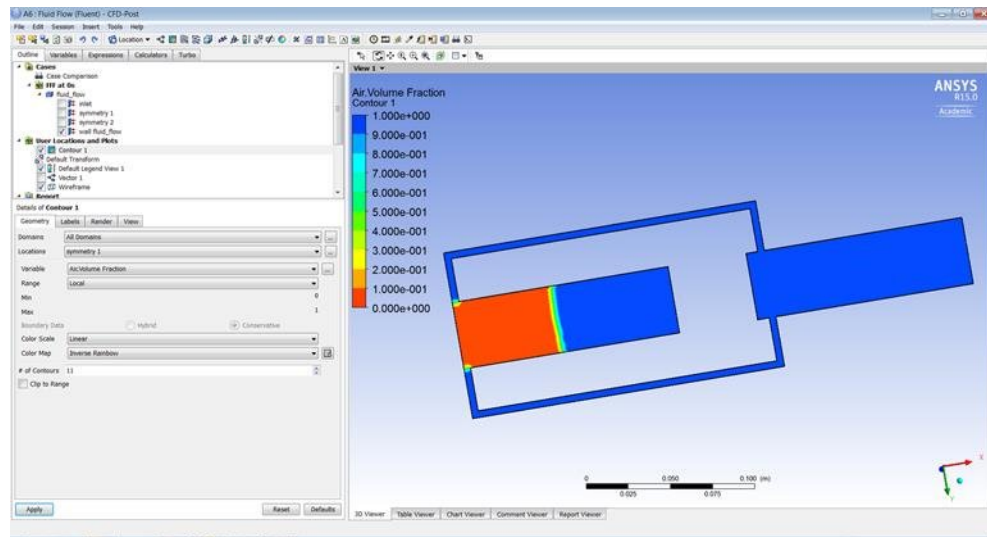
Figure 27 Simulation setup

6.5.   Cylindrical Tank with Round End Caps

Figure 28 shows the tank in pressure gradient at zero seconds, and it is made to spin at an angular speed of 14 rpm. The air inside the first tank is pressurized at 10 psi. In these conditions the flow is laminar. Figure 28 to 31 show evolution of the pressure

during the simulation.

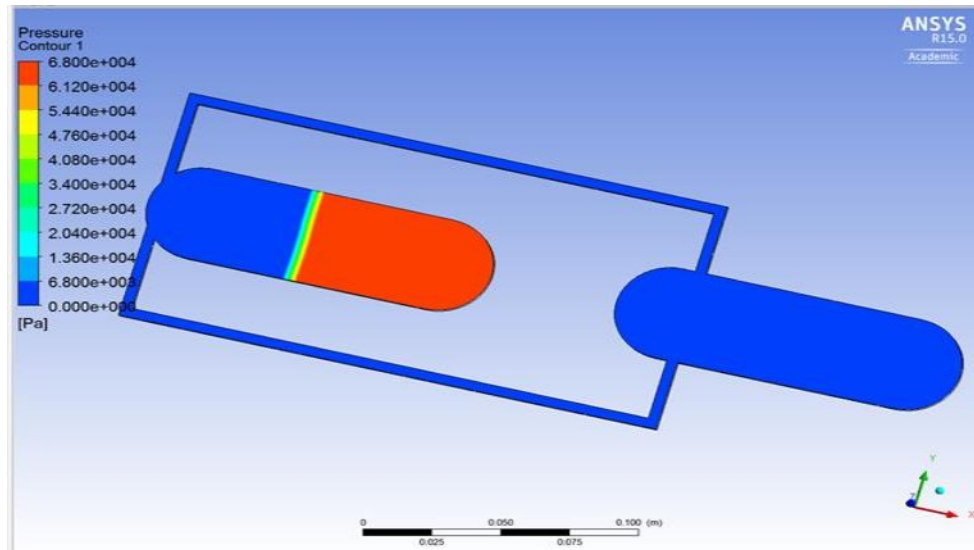Only the air in the first tank is pressurized.

Figure 28 Ansys result at T=0s

At T =0.025s (Figure 29) the pressure of the first tank decreases because of the expansion of air and the pressure in water increases because of the acceleration due to rotation.
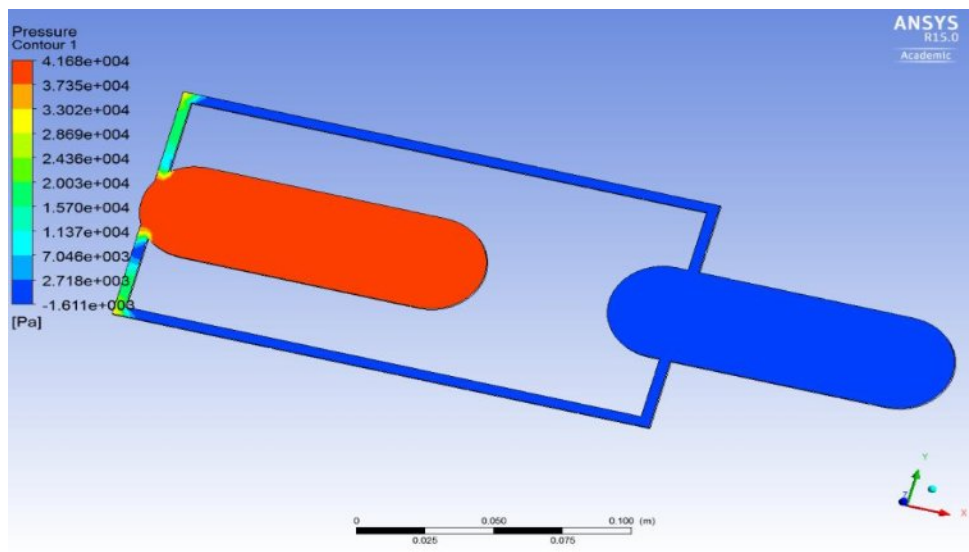
Figure 29 Ansys result at T=0.025s

At T=0.07s water moves in to the connecting lines and into to the second tank (Figure 30). The pressure is still decreasing in the first tank, and there is an increase in pressure in the second tank as the water flows in to it.
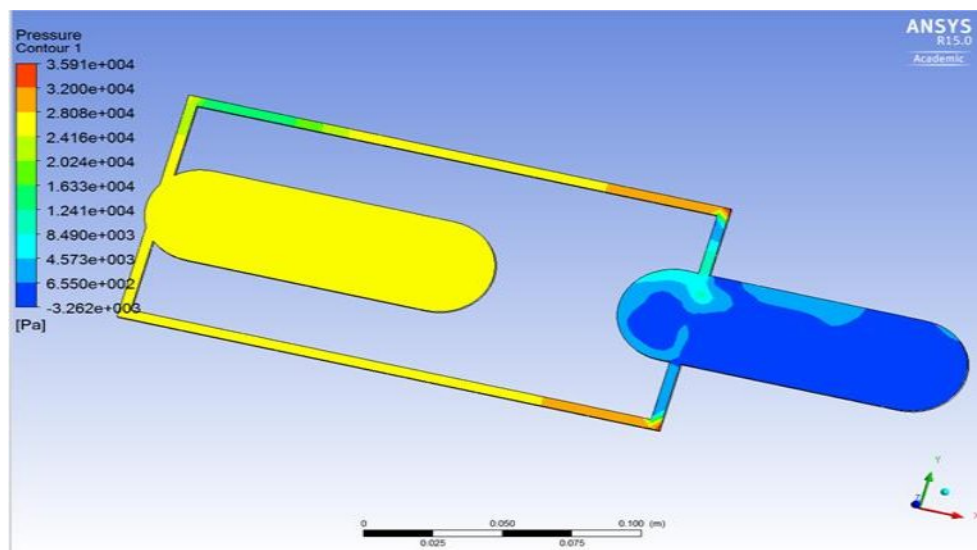
Figure 30 Ansys result at T=0.07s

At T=33s (Figure 31) the pressure in the first tank is further reduced, as the water is being transferred into the second tank. There is an increase in pressure in the second
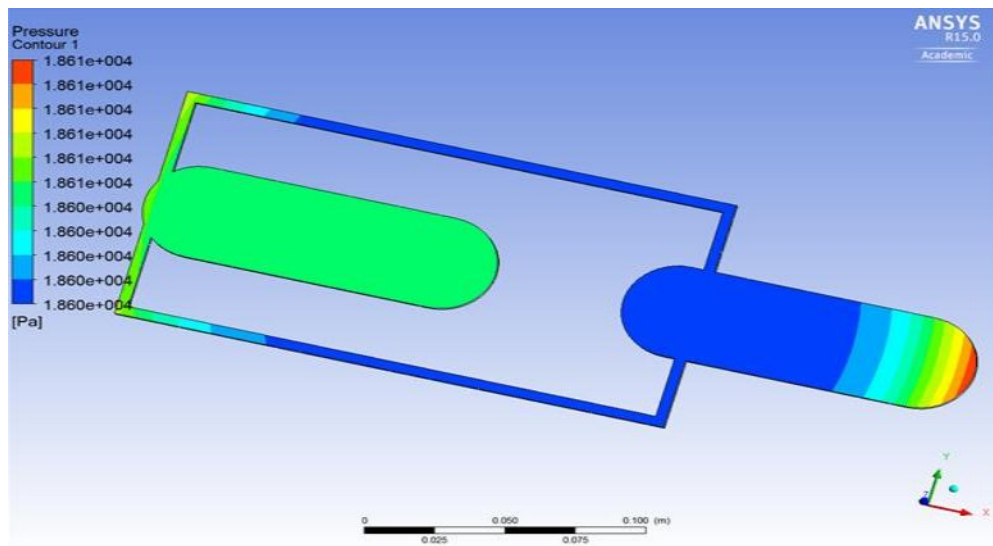
tank when the water flows in.

Figure 31 Ansys result at T=33s

Figure 32 to 36 show the evolution of the volume of air.

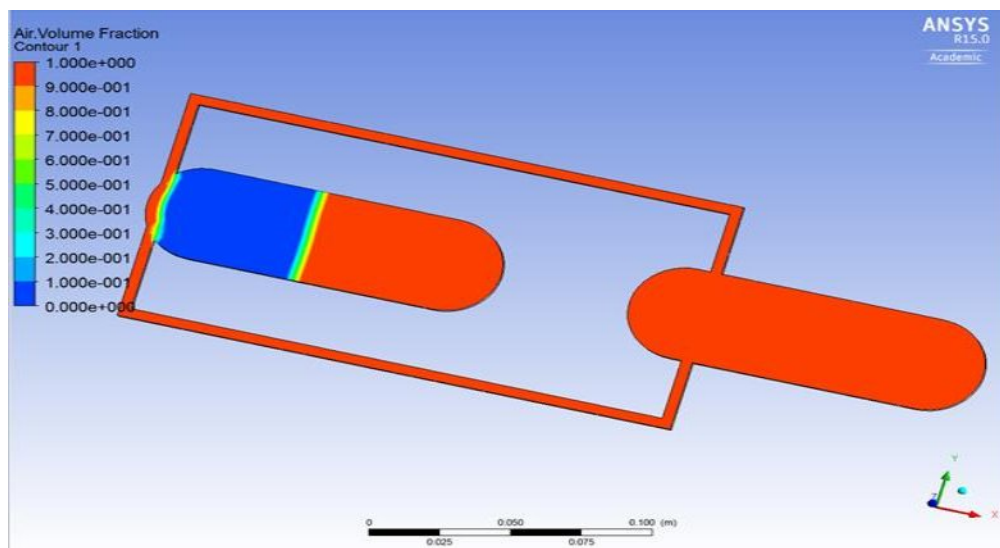At T=0s the first tank is half filled with water (Figure 32).

Figure 32 Ansys result at T=0s

T=0.035s

At T=0.035s water starts to move to the second tank through connecting lines because of the expansion of pressurized air.
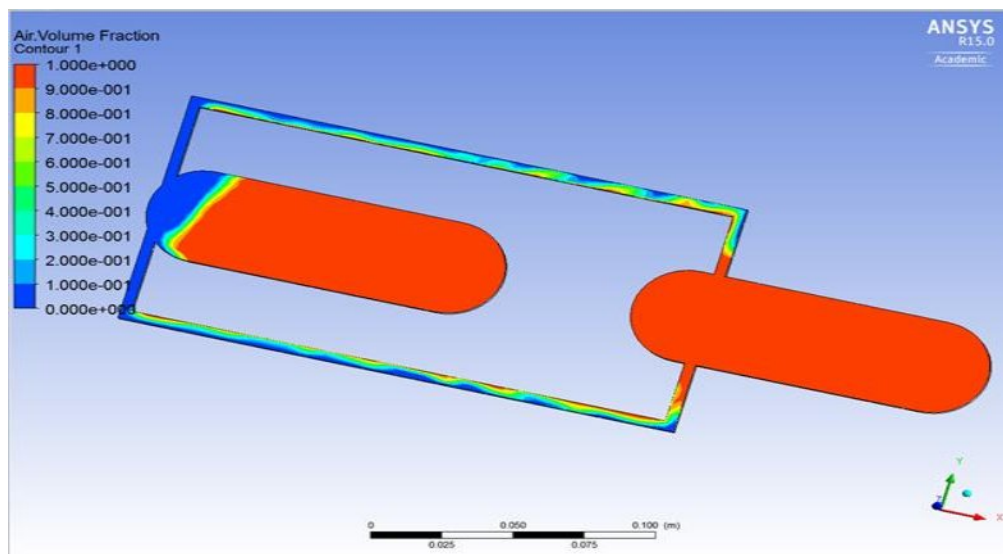

Figure 33 Ansys result at T=0.035s

T=0.25s

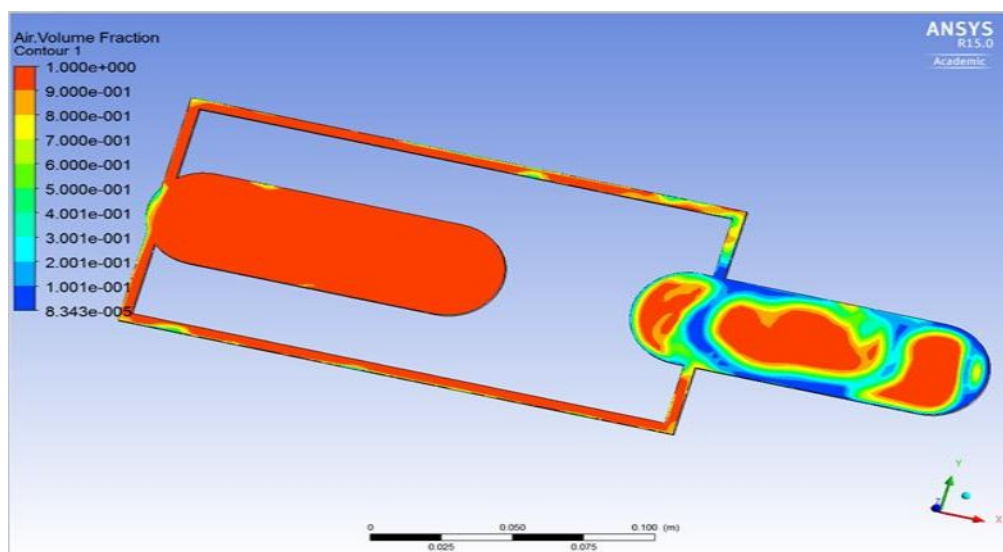At T=0.25s all the water is in the second tank but still there is some circulation area present.

Figure 34 Ansys result at T=0.025s

At T=2s some amount of water starts to return to the first tank (Figure 35). This could be due to circulation and low rotation speed.
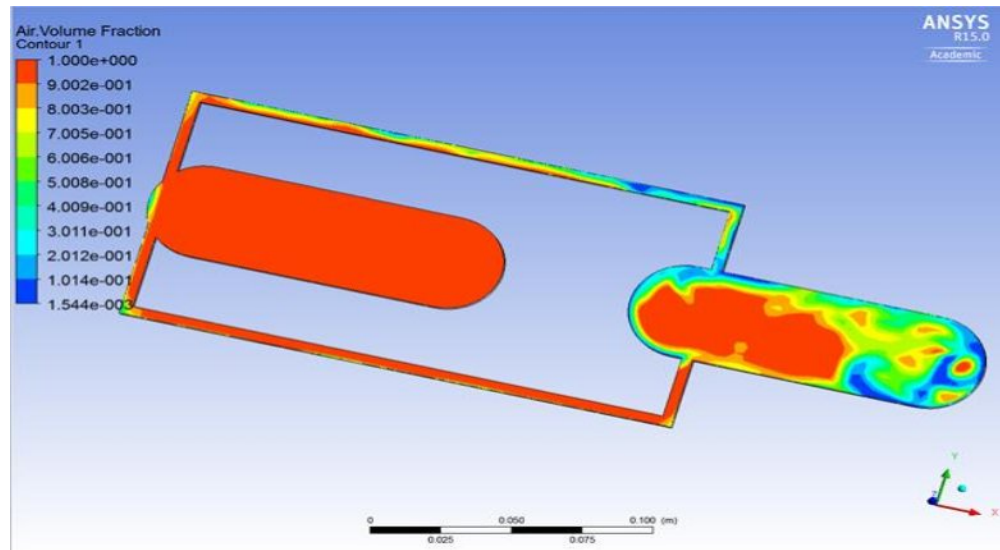

Figure 35 Ansys result at T=2s

T=33s

The system seems to be in a steady state. The water is localized at the edge of each tank due to centrifugal forces (Figure 36). There is a lot of surface where the volume fraction is around 0.5. The model for the interface may be changed.
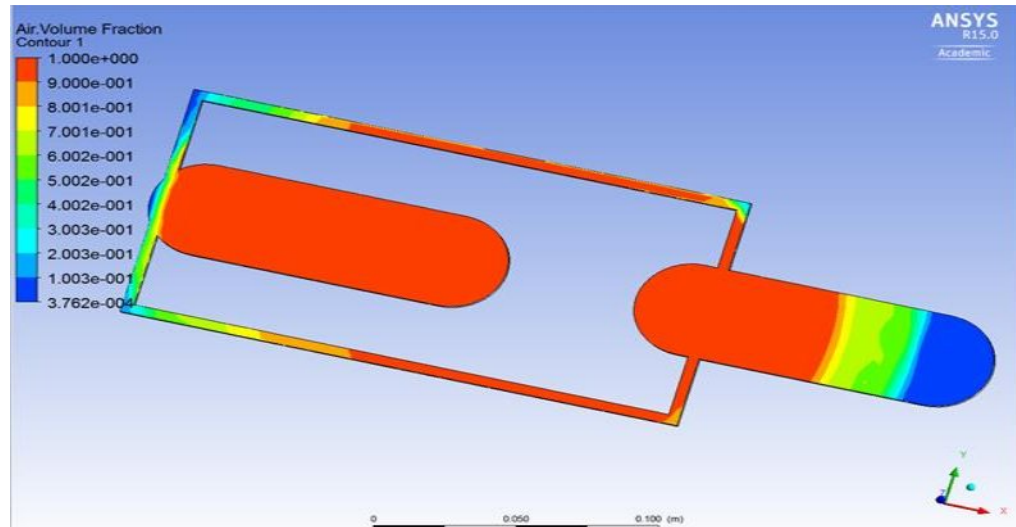
Figure 36 Ansys result at T=33s

6.6. Cylindrical Tank with Square End Caps

This system has a higher rotational velocity than the previously described setup. It spins around 20 rpm and has a turbulent flow. Figure 37 to 40 show evolution of the volume of air in the flow during the simulation.

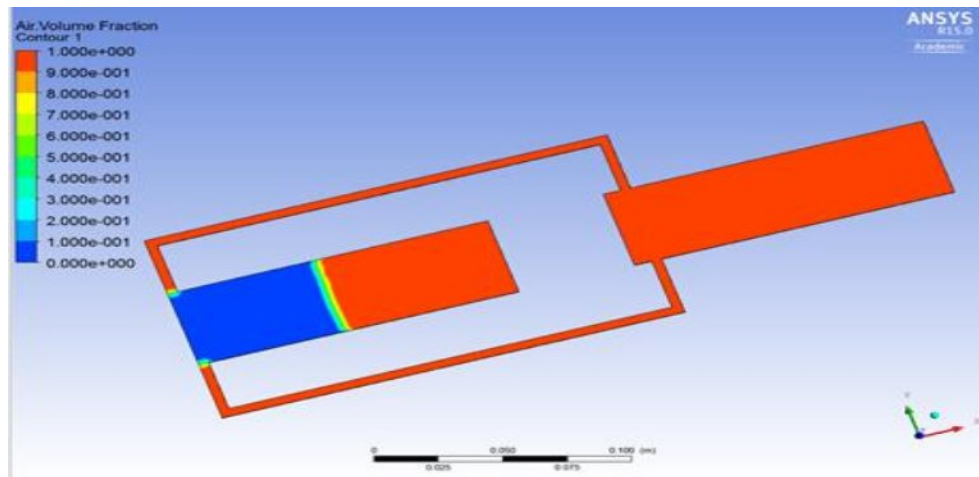Figure 37 shows the initial analysis set up for the flat end caps.

Figure 37 Ansys result at T=0s

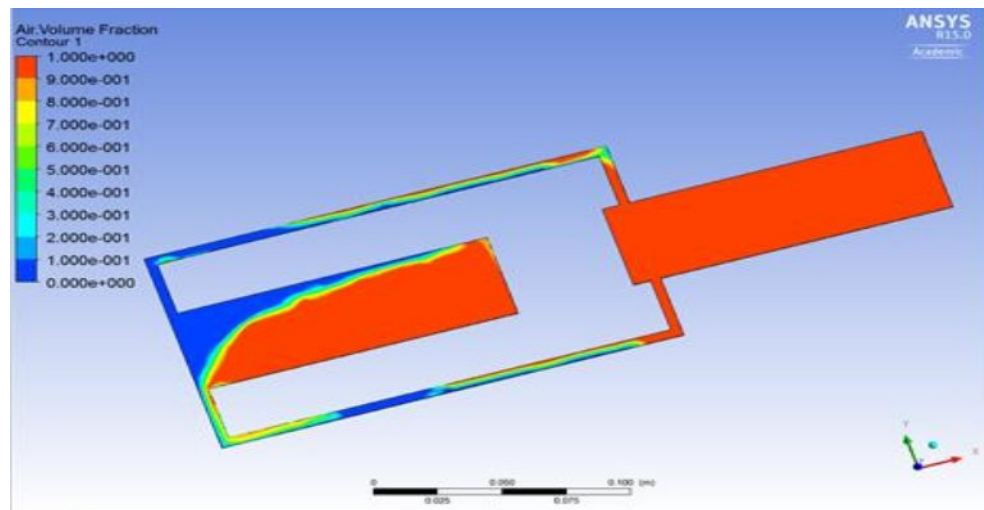At T=0.033s the fluid starts to flow through the tube (Figure 38)

Figure 38 Ansys result at T=0.033s

At T=0.122s almost all the liquid from the first tank flows into the second tank. The second tank experiences turbulence (Figure 39).
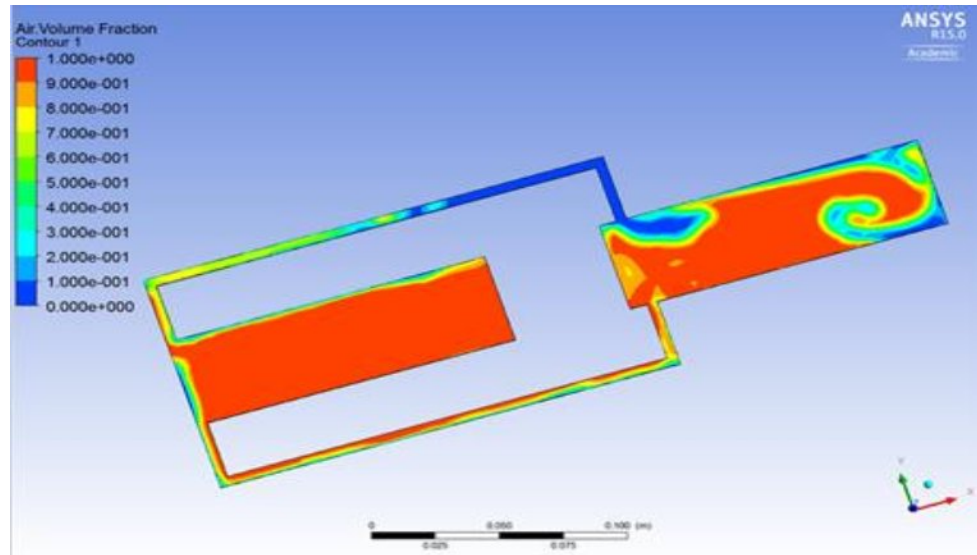
Figure 39 Ansys result at T=0.122s

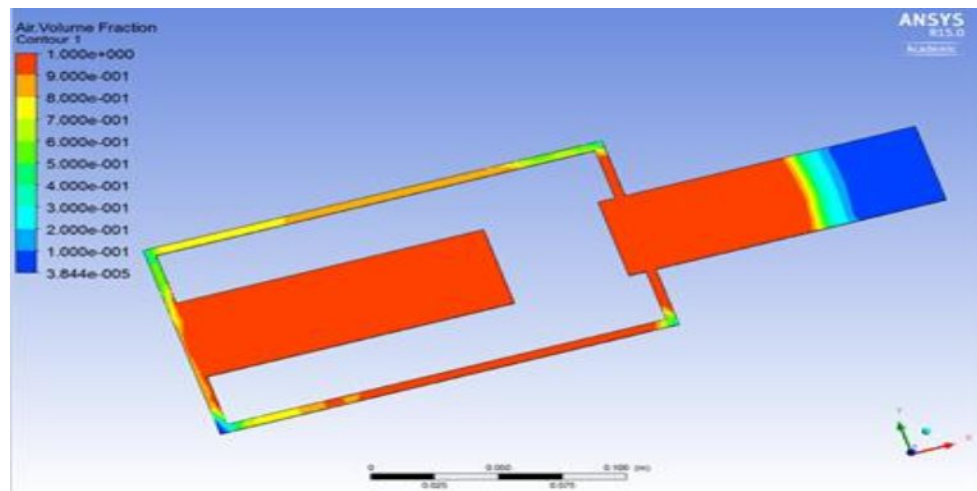At 3s the fluid in the second tank is settled and a small amount of fluid flows back to the first tank.

Figure 40 Ansys result at T=3s

The phenomenon is different from the previous transfer. The transfer is done faster and it seems to have less sloshes. But due to the high speed, there is more liquid at one side than the other.

7. CFD Analysis in STAR-CCM

7.1. Modeling the Tank in STAR-CCM

Previously flow transfer in ANSYS was performed. For better understanding of the flow behavior, CFD analysis in STARCCM is conducted. In this analysis, the tank design is changed for easy analysis purpose. Only the fill fraction of the tank is considered and meshed. This setup incorporates the curved caps of the tank.
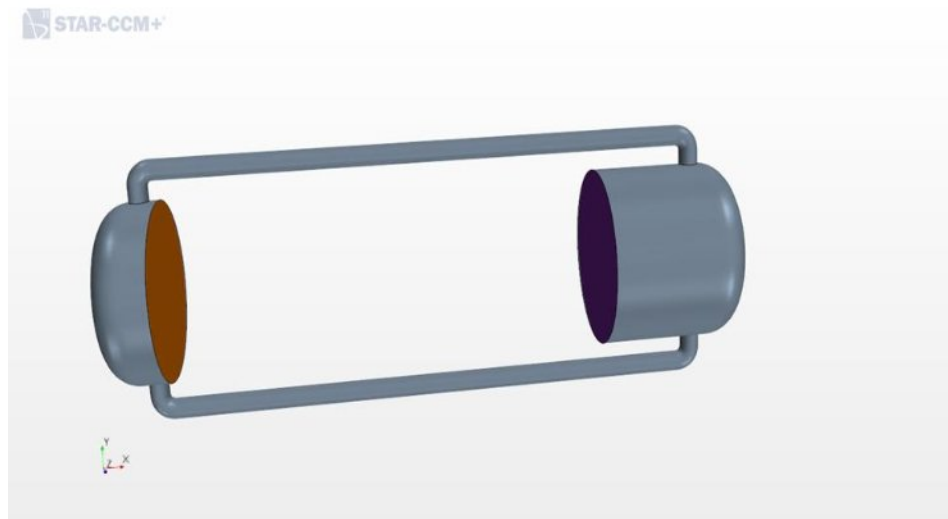
Figure 41 STAR-CCM model

7.2. Meshing Procedure

Mesh generally means the discretized representation of the portion involved in the domain of computation which is utilized by the physics in providing the numerical solution. Meshing is a critical component of any simulation. High quality mesh is required to get accurate results and provide solution convergence. But fine meshing would increase the computational time. Computation time also depends on the number of

iterations per unit time step and hence a relation should be established between the mesh and iterations for optimal results.

Physical time is the next most important factor that needs to be considered before the calculation. This establishes a relation between experimental setup and the simulation setup. Time step, number of iterations and mesh size should be chosen to obtain convergence solution, for the considered physical time while maintaining a low computational time. STARCCM has two types of meshing procedure, which is part based and regions based. These types of meshing procedure have their own advantage and disadvantage. For this simulation Regions based meshing is considered.
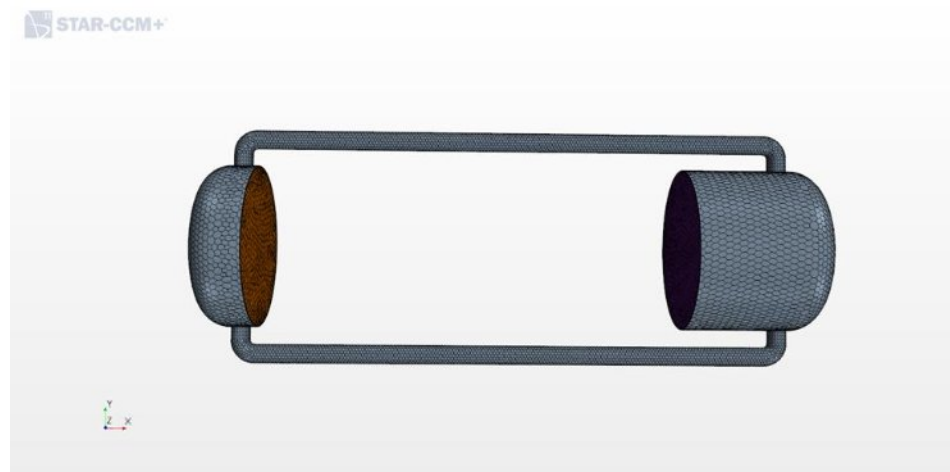

Figure 42 STAR-CCM model mesh
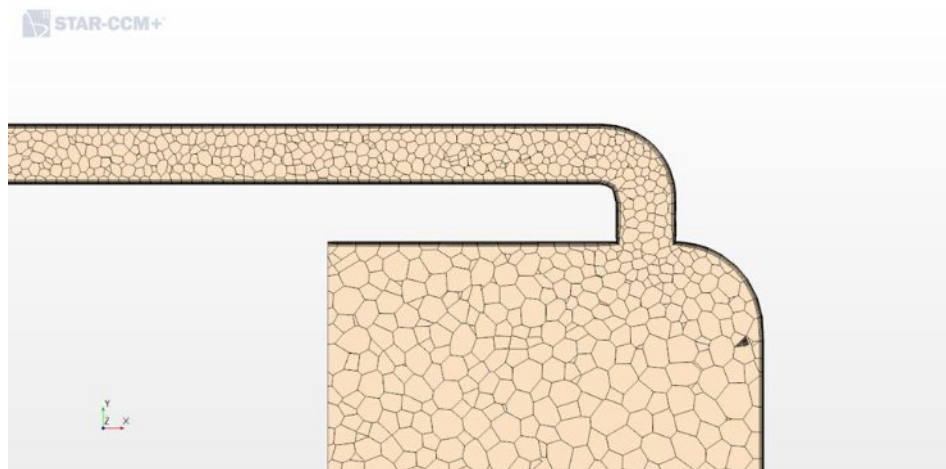
Figure 43 STAR-CCM model mesh (2)

7.3.   STAR-CCM Results

The propellant transfers from the small tank to the large tank indicating the fill fraction in supply tank. Only 30% of propellant is considered to be transferred to the receiver tank. For easier CFD analysis the receiver tank is considered to empty. Below are the results showing propellant behavior. The first result shows the pressure distribution along the tank and the transfer line. The next results show the velocity of the propellant flow rate.
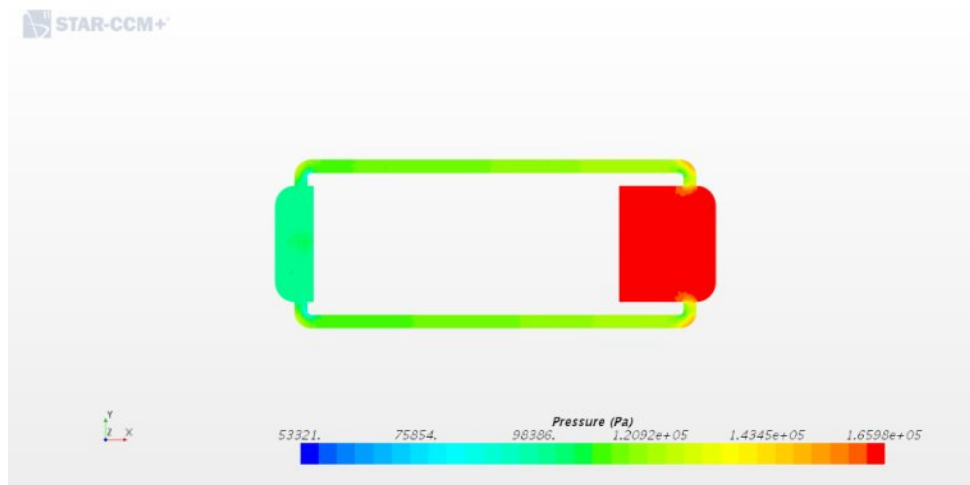
Figure 44 STAR-CCM result 1
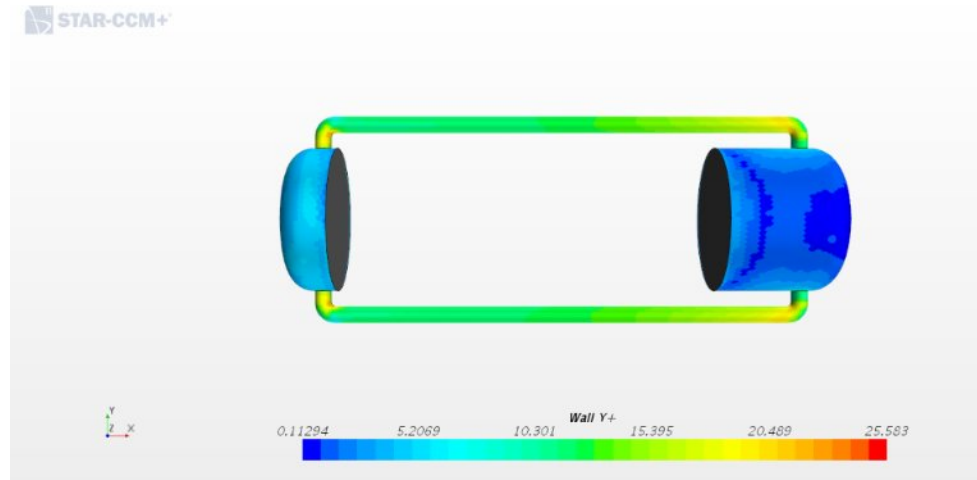
Figure 45 STAR-CCM result 2
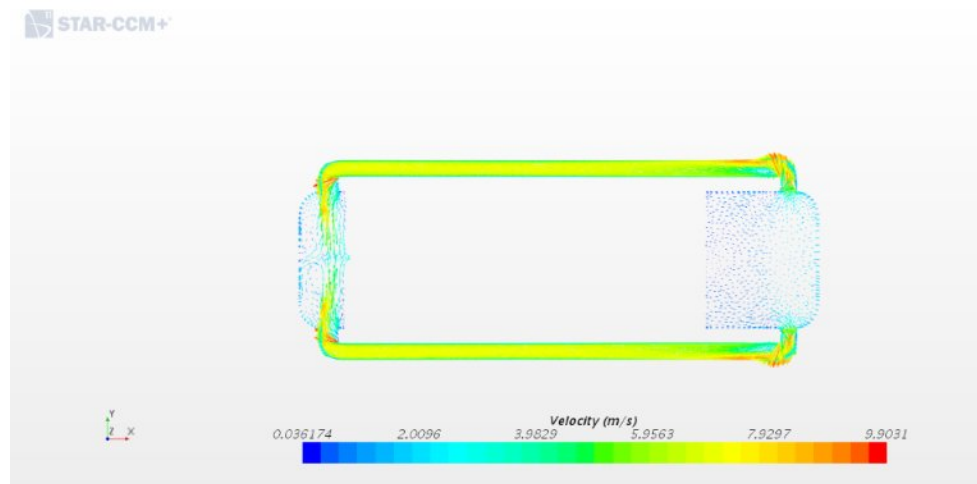
Figure 46 STAR-CCM result 3

7.4.   Computational Analysis Discussion

The above CFD analysis is performed to show the fluid reaction in earth conditions. For better understanding of the fluid flow, the CFD analysis needs to done more in-depth considering the fluid properties, fill fraction, settling acceleration, initial orientation, initial interface shape, settling criteria. The assumption made in this CFD analysis did not include liquid properties of a propellant. Anti-slosh baffles should be introduced into the tank to study the sloshing effects of the tank during the fluid transfer.

8. Conclusion

The concept of rotational transfer and storage of fuel in space is validated at Embry Riddle Aeronautical University. Stability dynamics of the system during the propellant transfer, mass gauging of amount of propellant in the tanks and finally the flow analysis of the transfer is carried out in CFD. From the stability analysis of the system it is seen that the system is stable but when propellant is being transferred the system becomes unstable. To make the system, stable again a counter balance system should be developed. Only the equation describing the counter balancing system is developed in this research. To develop the counter balancing system, the system the flow rate is of propellant is required. The flow rate of the propellant is calculated using Mass Gauging system. The mass gauging of the system is studied using experimental modal analysis. The experimental results from the mass gauging shows that, it is very effective. The transferred rate could not be determined accurately from this experimental model analysis, smaller sensors and more number of sensors are required to give more accurate results. Finally, the CFD analysis is performed to observe how the propellant would behave during transfer.

9. Future Work

The recommended future work of this research is to redesign the sensor placement and to increase the number of sensor inputs for more accurate data collection. Transfer rate of the propellant should be determined to design the counter balancing system. A more in-depth CFD analysis should be done considering the factors such as fluid properties, fill fraction, settling acceleration, initial orientation, initial interface shape, settling criteria. The assumption that is considered in the CFD analysis did not include liquid properties of the propellant. Also, Anti-slosh baffles should be introduced into the tank to study the sloshing effects of the tank during fluid transfer. The ground based experiment should be performed many times to ensure repeatability and consistency in the data obtained. Correlation of the numerical and experimental results and updating the system parameters through a system identification process should be developed.

REFERENCES

Grayson, G.D., 2003. Computational design approach to propellant settling. *Journal of spacecraft and rockets*, *40*(2), pp.193-200.

Bian, X., Perlin, M., Schultz, W. W., & Agarwal, M. (2003). Axisymmetric slosh frequencies of a liquid mass in a circular cylinder. Physics of Fluids (1994-present), 15(12), 3659-3664.

Chatman, Y, Gangadharan, S.N., Schlee, K., Sudermann, J., Walker, C., Ristow, J., Hubert, C., "Mechanical Analog Approach to Parameter Estimation of Lateral Spacecraft Fuel Slosh", 49th AIAA/ ASME/ ASCE/ AHS/ ASC Structures, Structural Dynamics, and Materials Conference, 2008

Devin Jr, Charles. "Survey of thermal, radiation, and viscous damping of pulsating air bubbles in water." The Journal of the Acoustical Society of America 31.12 (1959): 1654-1667.

Gangadharan, S. N. (2003). Parameter Estimation of Spacecraft Nutation Growth Model.

H. Nouri and F. Ravelet. Introduction à la simulation numérique des écoulements. Application au transfert thermique sur plaque plane avec StarCCM+. Arts ET Metiers ParisTech, 2013.

Hermann Schlichting and Klaus Gersten. Boundary-Layer Theory. Springer, 2000.

Kanda, Kimio. "Energy dispersive X-ray spectrometer." U.S. Patent No. 5,065,020. 12 Nov. 1991.

Kynan Maley. Best practices: Volume meshing. CD-adapco - South East Asian Conference, 2012.

Leuva, Dhawal, "Experimental Investigation and CFD Simulation of Active Damping Mechanism for Propellant Slosh in Spacecraft Launch Systems" (2011). Dissertations and Theses. Paper 91.

Loads, Propellant Slosh. "NASA Space Vehicle Design Criteria Monograph (Structures)." NASA SP-8009, August 1968.

Marsell, B., Gangadharan, S.N., Chatman, Y., Sudermann, J., Schlee, K., and Ristow, J., "A CFD Approach to Modeling Spacecraft Fuel Slosh", 47th AIAA Aerospace Sciences Meeting, Orlando, FL, 5-8 Jan. 2009

Marsell, B., Gangadharan, S., Chatman, Y., & Sudermann, J. (2009, May). Using CFD techniques to predict slosh force frequency and damping rate. In Proceedings of

5the 50th AIAA/ASME/ASCE/AHS/ASC Structures, Structural Dynamics and Materials Conference, Palm Spring, California (Vol. 22).

Mikell P. Groover and Emory W. Zimmers. CAD/CAM: Computer-Aided Design and Manufacturing. Prentice Hall, 1984.

Mouhamad, Malick, et al. "Physicochemical and accelerated aging tests of Metglas 2605SA1 and Metglas 2605HB1 amorphous ribbons for power applications." Magnetics, IEEE Transactions on 47.10 (2011): 3192-3195.

Neamțu, B. V., Geoffroy, O., Chicinaș, I., & Isnard, O. (2012). AC magnetic properties of the soft magnetic composites based on Supermalloy nanocrystalline powder prepared by mechanical alloying. Materials Science and Engineering: B, 177(9), 661-665.

Paul G. Tucker. Unsteady Computational Fluid Dynamics in Aeronautics. Springer, 2014.

Ramsay, Thomas N. "Floating absorber assembly for reduced fuel slosh noise." U.S. Patent No. 8,235,241. 7 Aug. 2012.

Rosario, L. P., Sivasubramanian, B., Das, S., & Gangadharan, S. (2016.)Active Damping of Fuel Slosh Using a Hybrid Magneto-Active Propellant Management Device. 54th AIAA Aerospace Sciences Meeting, AIAA SciTech, 4-8 January 2016, San Diego, California, USA

Ryu, Chulsung, Wooseok Seol, and Sangyeop Han. "Ablative baffle for a liquid rocket engine thrust chamber." U.S. Patent No. 7,036,303. 2 May 2006.

Samal, P. K., and J. B. Terrell. "Mechanical properties improvement of PM 400 series stainless steels via nickel addition." Metal Powder Report 56.12 (2001): 28-34.

Santhanam, Vijay, "Slosh DampingWith Floating Magnetoactive Micro-Baffles" (2014). Dissertations and Theses. Paper 181.

Sathya N. Gangadharan, "Parameter Estimation of Spacecraft Nutation Growth Model", H-1/H-4, John F. Kennedy Space Center, 2003.

Sivasubramanian, B., Rosario, L. P., Krishnappa, S., & Gangadharan, S. (2015). A Hybrid Magneto-active Propellant Management Device for Active Slosh Damping in Spacecraft. In 56th AIAA/ASCE/AHS/ASC Structures, Structural Dynamics, and Materials Conference (p. 1635).

Varas, David, Ramón Zaera, and Jorge López-Puente. "Numerical modelling of partially filled aircraft fuel tanks submitted to Hydrodynamic Ram." Aerospace Science and technology 16.1 (2012): 19-28

Vreeburg, J. P. (2005). Spacecraft maneuvers and slosh control. Control Systems, IEEE, 25(3), 12-16.

Wolf, Lance Alan. "Baffle for suppressing slosh in a tank and a tank for incorporating same." U.S. Patent No. 6,220,287. 24 Apr. 2001.

Crosby, K., Ireland, E., Lubick, K., Mathe, S., Metallo, S. and Werlink, R., 2014, August. A sounding rocket payload experiment on zero gravity fuel gauging using modal analysis. In Proceedings of the Wisconsin Space Conference.

Fortescue, P., Swinerd, G. and Stark, J. eds., 2011. Spacecraft systems engineering. John Wiley & Sons.

Larson, W.J. and Wertz, J.R., 1992. *Space mission analysis and design* (No. DOE/NE/32145--T1). Microcosm, Inc., Torrance, CA (US).

Boretz, J.E., 1970. Orbital refueling techniques. Journal of Spacecraft and Rockets, 7(5), pp.513-522.

Wertz, J.R. ed., 2012. Spacecraft attitude determination and control (Vol. 73). Springer Science & Business Media.

Equation 1:

$$\bar{x}_x =$$

$$\frac{m_{tank1}\left(d_1 - \frac{l_{tank1}}{2}\right) + m_{tank1}\left(d_2 + \frac{l_{tank2}}{2}\right) + m_{connecting}\left(\frac{l_{connecting}}{2}\right) + (m_{fluid1} - \dot{m}_{transfer}t)\left[(d - l_{tank1}) + \frac{(m_{fluid1} - \dot{m}_{transfer}t)}{2 * \rho_{fluid} * \pi * r_{tank1}^2}\right] + (m_{fluid2} - \dot{m}_{transfer}t)\left[(d + l_{tank2}) - \frac{(m_{fluid2} - \dot{m}_{transfer}t)}{2 * \rho_{fluid} * \pi * r_{tank2}^2}\right]}{m_{tank1} + m_{tank2} + m_{connecting} + (m_{fluid1} - \dot{m}_{transfer}t) + (m_{fluid2} - \dot{m}_{transfer}t)}$$

Equation 2:

$$\bar{\bar{x}}_x =$$

$$\frac{m_{tank1}\left(d_1 - \frac{l_{tank1}}{2}\right) + m_{tank1}\left(d_2 + \frac{l_{tank2}}{2}\right) + m_{connecting}\left(\frac{l_{connecting}}{2}\right) + (m_{fluid1} - \dot{m}_{transfer}t)\left[(d - l_{tank1}) + \frac{(m_{fluid1} - \dot{m}_{transfer}t)}{2 * \rho_{fluid} * \pi * r_{tank1}^2}\right] + (m_{fluid2} - \dot{m}_{transfer}t)\left[(d + l_{tank2}) - \frac{(m_{fluid2} - \dot{m}_{transfer}t)}{2 * \rho_{fluid} * \pi * r_{tank2}^2}\right] + m_w\left(r + \frac{l_w}{2}\right)}{m_{tank1} + m_{tank2} + m_{connecting} + (m_{fluid1} - \dot{m}_{transfer}t) + (m_{fluid2} - \dot{m}_{transfer}t) + m_w}$$

Equation 3:

$$m_w =$$

$$\frac{m_{tank1}\left(d_1 - \frac{l_{tank1}}{2}\right) + m_{tank1}\left(d_2 + \frac{l_{tank2}}{2}\right) + m_{connecting}\left(\frac{l_{connecting}}{2}\right) + (m_{fluid1} - \dot{m}_{transfer}t)\left[(d - l_{tank1}) + \frac{(m_{fluid1} - \dot{m}_{transfer}t)}{2 * \rho_{fluid} * \pi * r_{tank1}^2}\right] + (m_{fluid2} - \dot{m}_{transfer}t)\left[(d + l_{tank2}) - \frac{(m_{fluid2} - \dot{m}_{transfer}t)}{2 * \rho_{fluid} * \pi * r_{tank2}^2}\right]}{\left(r + \frac{l_w}{2}\right)}$$

Equation 4:

$$r = \left(\frac{m_{tank1}\left(d_1 - \frac{l_{tank1}}{2}\right) + m_{tank1}\left(d_2 + \frac{l_{tank2}}{2}\right) + m_{connecting}\left(\frac{l_{connecting}}{2}\right) + (m_{fluid1} - \dot{m}_{transfer}t)\left[(d - l_{tank1}) + \frac{(m_{fluid1} - \dot{m}_{transfer}t)}{2 * \rho_{fluid} * \pi * r_{tank1}^2}\right] + (m_{fluid2} - \dot{m}_{transfer}t)\left[(d + l_{tank2}) - \frac{(m_{fluid2} - \dot{m}_{transfer}t)}{2 * \rho_{fluid} * \pi * r_{tank2}^2}\right]}{m_w}\right) - \frac{l_w}{2}$$

A.   Mat Lab Code

```matlab
function  peak = FFTTest(name)


[~, ~, X] = xlsread(name);
%{
Data in each row
1-6 Unused
7 Sample rate
8-18 Unused
19 Data points
20 Data Zero
21-24 Unused
25-end  Data
%}
%Get usefull data from the cell
SampleRate = X{6,2};
Length = X{19,2};
ZeroData = X{20,2};
Data = cell2mat(X(24:end,1:3));
Time = Data(:,1);
Voltage = Data(:,2);
Voltage2 = Data(:,3);
Period = 1/SampleRate;
Length = length(Voltage);

%Find the next power of two closest to the length
NFFT = 2^nextpow2(Length);

%Perform FFT on the data
fftVoltage = fft(detrend(Voltage), NFFT);
fftVoltage2 = fft(detrend(Voltage2), NFFT);

%Extract the real part of the FFT
OneSpec = abs(fftVoltage)/NFFT;
OneSpec2 = abs(fftVoltage2)/NFFT;

%Calculate the Response Function;
Spec = OneSpec./OneSpec2;

%Calculate the frequency domain
Freq = SampleRate/2*linspace(0,1,NFFT/2+1);
Cutoff = find(Freq == 5000);
FreqPlot = Freq(1:Cutoff);

%Find the one-sided spectrum
SpecPlot = Spec(1:Cutoff);
OneSpec = OneSpec(1:Cutoff);
OneSpec2 = OneSpec2(1:Cutoff);

magnitude = max(SpecPlot);
tf = (SpecPlot == magnitude);
peak = FreqPlot(tf);
```

```matlab
% info = sprintf('Peak: %.3f\nMagnitude: %.3f', peak, magnitude);

%Plot
%Plot the raw data
h = figure('Position', [250 10 1250 750]);
subplot(3,2,1)
plot(Time,Voltage)
title('Raw Data');
axis tight
grid on
xlabel('Time (msec)');
ylabel('Voltage 1 (mV)');
subplot(3,2,2)
plot(Time,Voltage2)
title('Raw Data');
axis tight
grid on
xlabel('Time (msec)');
ylabel('Voltage 2 (mV)');
subplot(3,2,3)
plot(FreqPlot, OneSpec)
title('FFT result 1');
xlabel('Frequency (Hz)');
ylabel('Amplitude');
grid on
subplot(3,2,4)
plot(FreqPlot, OneSpec2)
title('FFT result 2');
xlabel('Frequency (Hz)');
ylabel('Amplitude');
grid on
subplot(3,2,5)
plot(FreqPlot, SpecPlot)
title('Frequency Response');
xlabel('Frequency (Hz)');
ylabel('Amplitude');
grid on
% x = 0.8*FreqPlot(length(FreqPlot));
% y = 0.8*max(SpecPlot);
% text(x,y,info);
end
```